Atomic scattering of H and N on W(100): Effect of lattice vibration and electronic excitations on the dynamics

C. Ibarguen Becerra, C. Crespos, O. Galparsoro, P. Larregaray

Atomic scattering of H and N on W(100): effect of lattice vibration and electronic excitations on the dynamics

C. Ibarguen Becerra,[1,2] C. Crespos,[1,2,a)] O. Galparsoro,[3,4] and P. Larregaray[1,2]
[1)] *Université Bordeaux, ISM, UMR5255, F-33400 Talence, France*
[2)] *CNRS, ISM, UMR5255, F-33400 Talence, France*
[3)] *Institute for Physical Chemistry , Georg-August University of Göttingen, Tammannstr. 6, 37077 Göttingen, Germany*
[4)] *Department of Dynamics at Surfaces, Max-Planck Institute for Biophysical Chemistry, Am Faßberg 11, 37077 Göttingen, Germany*

(Dated: 12 June 2020)

Scattering of H and N atoms from W(100) surface has been theoretically studied by means of classical trajectories based on an electronically adiabatic potential energy surface (PES). The PES has been constructed by interpolation of density functional theory (DFT) calculations following a corrugation reducing procedure (CRP). Van der Waals interactions are taken into account by using the vdW-DF2 exchange- correlation functional. In the dynamics a special focus is made on the influence of energy release through surface atoms motion and electrons of the metal. Most part of the H-atoms sticking is mediated through penetration into the sub-surface area where electron-hole pairs excitation plays the major role. For N-atoms the sticking is mainly due to the coupling with lattice vibrations, as expected when considering heavy atoms. Adsorption and absorption processes have been characterized for both H/W(100) and N/W(100) exhibiting differences between those benchmark light and heavy atoms in interaction with metals.

Keywords: Dynamics of atomic scattering on surfaces, theoretical simulations, quasi-classical trajectories, van der Waals forces.

I. INTRODUCTION

The scattering of atomic species on metal surfaces is of high interest in many domains of fundamental and applied science as for example heterogeneous catalysis[1–7], plasma-wall interactions in nuclear physics[8–11], or for the aerothermochemistry of thermal protection systems in atmospheric reentries[12–30]. A key question to address is the release of energy into the surface by means of coupling between the translational degrees of freedom of the atom and the surface atoms motion or the electrons of the solid[31–35]. H-atom sticking, after single or multiple collisions with the surface, has been shown to occur mainly through loss of energy due to electron-hole (e-h) pairs excitations[33,36–42]. Because of the large mass mismatch between atoms of the metal and hydrogen, transfer of energy to the lattice vibrations is unlikely to occur. Recent experimental and theoretical works on H-atom collision with several (111) surfaces of *fcc* transition metals (Au, Pt, Ag, Pd, Cu, and Ni) have exhibited a universal behavior with respect to nonadiabatic adsorption processes[41]. In this work, authors have shown that energy loss is almost independent of the metal and is mainly due to electronic friction. Since no influence of metals work functions is observed, authors also conclude that no charge transfer occurs between the impinging atom and the surface upon collision for an initial energy of 1.92 eV.

In this work, simulations have been performed on the H/W(100) benchmark system leading to a further analysis of the universal energy loss scheme proposed by Dorenkamp *et al.* in the context of a more open surface and a *bcc* metal. Moreover, the penetration of atomic hydrogen on W metal is of high interest in the context of nuclear physics[43–47]. As a matter of fact, the study of H scattering in tungsten has gained a lot of interest in the last decades in the context of plasma facing materials (PFMs)[43–47], in which tungsten is a promising candidate. Hydrogen is known to induce blisters formation when tungsten is exposed to the high flux plasma irradiation, specially at low incident energy.[48] It is also known that blistering problem induced by H retention may cause reduction of the lifetime of the material. Consequently, a discussion of first step H absorption and scattering into the solid is proposed, pointing out the importance of electronic friction for the description of sub-surface atoms motion.

For heavier atoms, such as nitrogen, energy exchange with lattice vibration are expected to be much more efficient. Scattering dynamics simulations are here also performed for N/W(100). Again, energy dissipation channels are included in the simulations addressing the question of the competition between both e-h pairs and lattice vibration excitation upon heavy atoms sticking on a metal surface[49–51]. Coupling between the normal and parallel motion of the N atoms mediated through corrugation has been shown to play a role[52,53] especially at low collision energy. A special focus on this issue is made in this work, by revisiting the early work of G. Volpilhac *et al.*[52,53] where no energy loss channels were included in the simulations.

A new potential energy surface (PES) has been built for H/W(100) by interpolation of density func-

[a)] cedric.crespos@u-bordeaux.fr

tional theory (DFT)[54,55] calculations making use of the vdW-DF2[56] exchange correlation functional. For the N/W(100), we have used a similar PES, developed and presented elsewhere[57,58]. The choice of the functional was originally motivated by previous works suggesting that dispersion forces may play an important role in the dynamics of molecules in interaction with metal surfaces[57–60]. However, comparing the vdW-DF2 based PESs with older ones calculated at PW91 level, no significant differences has been noticed for the particular cases of both N/W(100) and H/W(100). We have checked that the dynamics is almost unaltered by the choice of the functional in the energy range we consider in this work.

The paper is organized as follows: In Section II the computational details and methodology are presented. Results are discussed in Section III and a summary with the main conclusions is given in Section IV.

II. COMPUTATIONAL DETAILS

The interaction between H and N atoms with the W(100) surface has been modelled by a 3-dimensional PES which depends on X, Y, and Z coordinates referring the position of the H/N atom with respect to one surface atom at the origin of the Cartesian frame. The X and Y are along the sides of the square unit cell. In order to get a continuous 3D-PES a Corrugation reducing procedure (CRP)[61–63] has been used to interpolate a set of about 900 DFT single point calculations. A grid of 60 Z values above 15 sites of the surface have been sampled (see Fig. 1 for details).

A periodic supercell approximation has been used. The metallic surface is represented by a 5-layer slab, and the calculations were performed using a 15x15x1 Monkhorst-Pack grid of k points for a (2x2) structure. We obtained a bulk lattice constant of $a = 3.239$ Å. After relaxation, an interlayer distance of $0.437a$ has been found for the two topmost layers and of $0.517a$ between the second and the third layer. Spin-polarized DFT calculations have been carried out within the Generalized Gradient Approximation (GGA)[64,65] making use of the vdW-DF2[56] exchange-correlation functional. Ultrasoft pseudo-potentials[66–68] have been used to describe the interaction with atomic cores. All the calculations were performed with the Vienna Ab Initio Simulation Package (VASP)[69–73]. The 3-dimensional PES for H/W(100) has been built in the framework of this investigation, while the N/W(100) PES has been taken from the work of A. Pena-Torres et *al*[57].

The dynamics simulations are based on the adiabatic 3D-PESs making use of the classical trajectories method. In order to calculate probabilities for the different exit channels such as adsorption, absorption and/or reflection, 10000 trajectories have been performed for several initial collision energies ranging from 10 meV to 5.0 eV. The initial X and Y positions of the atoms above the W(100) unit cell were randomly selected leading to uniform sampling. All trajectories have been started at

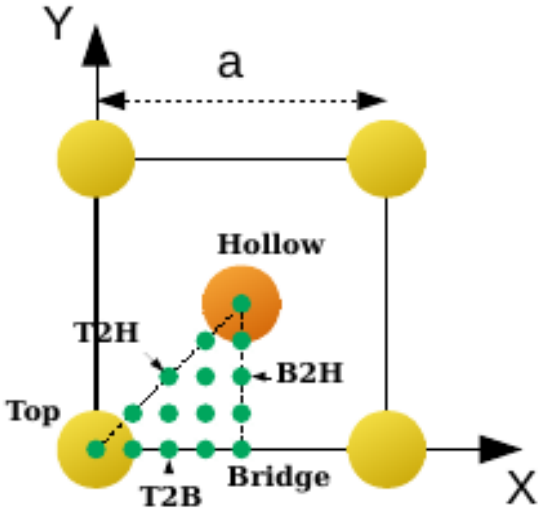

FIG. 1. Top-view of the unit cell and the sites (green points) for which DFT calculations have been carried out. W atoms in the first layer are in yellow. In orange W atom belongs to the second layer. Top, Bridge, Hollow, Top-to-Bridge (T2B), Top-to-Hollow (T2H), and Bridge-to-Hollow (B2H) high symmetry sites are shown. The lattice constant is $a = 3.239$ Å.

$Z_0 = 6.0$ and $Z_0 = 7.0$ Å from the surface in the asymptotic region of the PES for H and N atoms, respectively. Normal and off-normal incidence conditions have been analyzed. An atom is considered as reflected whenever it reaches back its initial distance from the surface Z_0 with a velocity pointing towards vacuum. Absorption occurs when atoms reach the value of $Z_{min} = -3.0$ Å which corresponds to a position slightly above the third layer of the slab. The atoms are also considered as absorbed if, after the maximum integration time of 2.0 ps, they remain between the top layer ($Z = 0$) and the third layer ($Z_{min} = -3.0$ Å) with kinetic energy lower than the one required to escape from the bulk. Adsorption occurs when the atom is neither reflected nor absorbed with a kinetic energy lower than the minimum required to escape the attractive potential of the surface. The maximum integration time of 2.0 ps has been chosen such that the exit channel probabilities are all converged.

In the calculations, a surface oscillator was used to simulate energy exchange between the atom and vibrations of the lattice via the so-called generalized Langevin oscillator (GLO) model[34]. Individual motions of surface atoms are not treated explicitly within the GLO model, thus lattice motion effects are accounted for in a very approximate way. Theoretical simulations performed by F. Nattino et al.[74] on N_2/W(110) system, have shown that despite its simplicity, the GLO model is able to capture the physics of the problem. For instance, N_2 dissociation probability on W(110) calculated at GLO level compares well with probability evaluated through more elaborated treatment such as Ab Initio Molecular Dynamics (AIMD) method. Moreover, those two methods predict very sim-

ilar energy transfer between the molecule and the lattice degrees of freedom for the case of non-reactive scattering events. Then energy dissipation to the metal mediated by e-h pairs excitations is modelled by an effective friction term introduced in the classical equations of motion, and evaluated through the Local density friction approximation (LDFA)[35,51]. Previous works on H scattering on various metals have excluded any formation of a transient H^- specie since energy loss spectra have been shown to be mostly independent of the work function of metals[41]. Thus, electronic excitations only treated at the LDFA level are expected to quantify correctly the energy loss of the atoms in interaction with the surface electron density.

III. RESULTS AND DISCUSSION

Analysis of the PES

In order to describe the main features of the PESs for the two systems under study, i.e., H/W(100) and N/W(100), 1D cuts of the potentials for the highest symmetry surface sites as a function of altitude Z are displayed in Fig. 2.

H/W(100)

In agreement with previous experimental and theoretical works[75–77], the bridge site is the most stable site for H adsorption on W(100) at $Z = 1.11$ Å with a 3.08 eV binding energy. The penetration of the H atom into the slab is energetically favorable through the bridge site with barriers below the asymptotic potential energy. At large distances (between 2.0 and 3.0 Å) the top site is the most attractive site. On Fig. 2, three sites of absorption have been identified and labeled as 1, 2, and 3. We have checked that each of those sites corresponds to true minima of the 3D-PES by visualizing 2D-cuts as a function of X and Y coordinates for the different Z values of the 3 sites.

N/W(100)

For N/W, the most stable site is the hollow at $Z = 0.63$ Å with a 6.75 eV binding energy, rather similar to that of the B2H site, in agreement with previous results reported for Volpilhac et *al*[52]. The absorption process is shown to be activated with a barrier height of about 2 eV on the bridge (with respect to the origin of the potential energy that is set for N far from the surface), whereas the top site remains as the most attractive site at large distances, like in the H/W case.

For both H/W and N/W a comparison with previous PESs based on PW91 functional has been made and, in contrast to what was found for N_2,[57,78] for instance, no significant changes have been noticed by adding van der Waals contributions to the description of atom-surface interaction. This result may be due to the rather weak polarizability of the H and N atoms.

Sticking Probability

The total sticking probability S_0, defined as $S_0 = 1 - P_{ref}$ with P_{ref} being the atomic reflection probability, is plotted in Fig. 3 as a function of initial collision energy (E_i). Results for both H and N + W(100) are included. A comparison is made between the sticking probabilities calculated using three models previously described: (i) the static surface approximation (Born-Oppenheimer static surface - BOSS) for which no exchange of energy is accounted for, (ii) the GLO model to allow energy dissipation to lattice vibrations and account for surface temperature (here 300K) (iii) the GLO-LDFA model in which both surface motion and *e-h* pairs excitations are accounted for in the simulations (GLO-LDFA). By comparing the three models, it is possible to infer which dissipation channel dominates energy transfer to the surface.

From the information contained in Fig. 3 arises that, within the BOSS model, the sticking probability of H decreases sharply when the initial collision energy increases to approximately 200 meV and then remains almost constant up to 1 eV. In the case of N/W, S_0 decreases monotonically throughout the range when energy is increased, as has been observed in earlier theoretical simulations,[52] where it has been shown that dynamic trapping governs the sticking of atoms at low energy. Within the BOSS level, only transfer of energy between the perpendicular and parallel motion of the atom can lead to trapped atoms. By increasing collision energy this transfer becomes rapidly inefficient and the sticking probability gets small. At this level of approximation, one may compare the present BOSS results with the ones obtained by Volpilhac *et al*[52] on a PW91 based PES, for collision energy going from 10 meV to 1 eV. In their study, absorption was supposed to occur whenever trajectories were able to reach the top surface layer located at $Z = 0$. Then, the calculation was stopped and those trajectories were accounted for in the sticking probability. For comparison purposes, we have performed a calculation of the sticking probability using the same criteria. An almost identical sticking curve is obtained with a sharp decrease and a plateau at about 0.5. If atoms are allowed to travel between $Z = -3.0$ and 0 Å in the simulations, the sticking probability is largely reduced (with a value of 0.1 for 1 eV of collision energy (see Fig. 3) and composed uniquely of long-lived species bouncing on the surface with high kinetic energy. This result shows that resurfacing[37] and sub-surface motion plays an important role in the dynamics and should be accounted for in the simulations.

Going beyond the BOSS model by including energy dissipation channels increases significantly the trapping of atoms within the energy range considered in Fig. 3 and previous studies of Volpilhac *et al.*[52], i.e., 10 meV $\leqslant E_i \leqslant$ 1 eV. A comparison of the GLO and GLO-LDFA curves

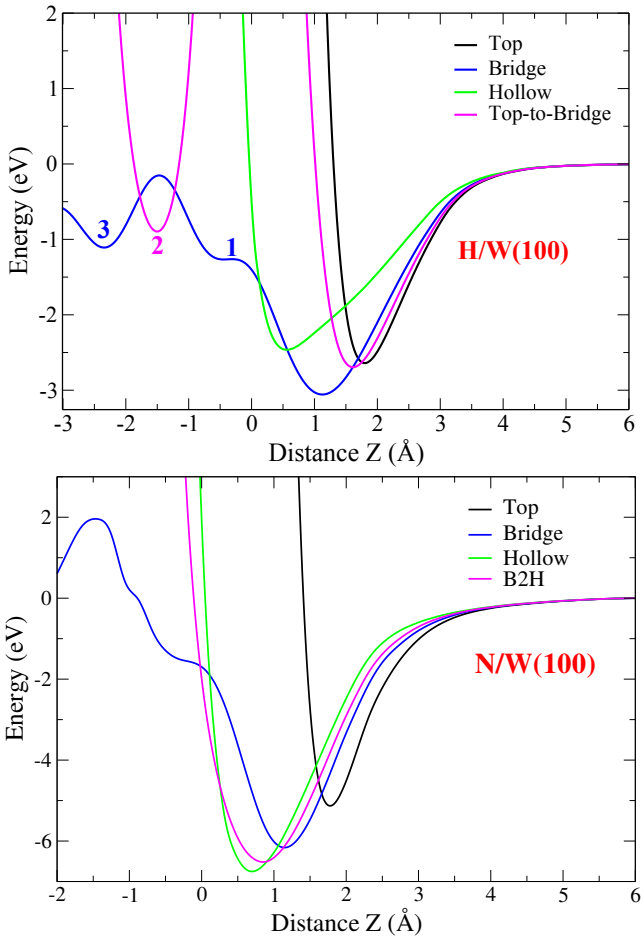

FIG. 2. 1D cuts of the potential energy surface as a function of atom/surface distance Z for several high symmetry sites. The upper panel corresponds to H/W(100) systems. 1, 2, 3 refers to absorption sites. The lower panel corresponds to N/W(100). Energies and distances are given in eV and Å, respectively.

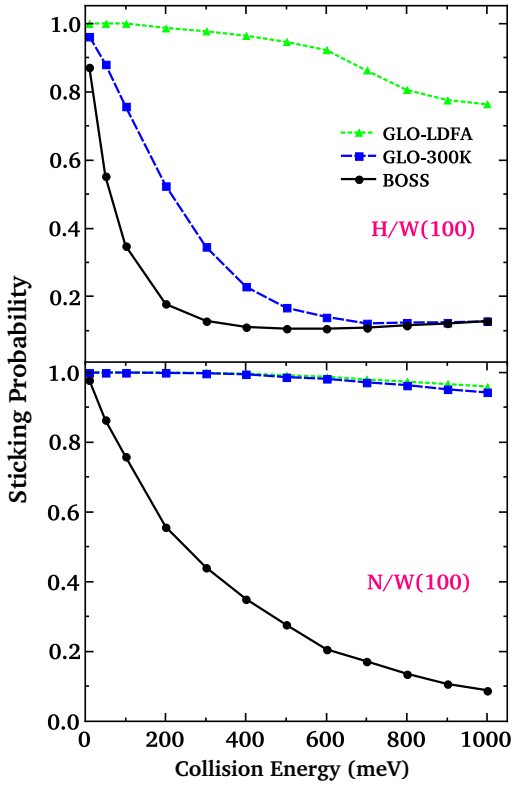

FIG. 3. Sticking probabilities as a function of atomic collision energy for H/W(100) (upper panel) and N/W(100) (lower panel). A comparison is made between simulations with no energy dissipation channels (BOSS), only phonons (GLO 300 K) and both phonons and electronic dissipation channels (GLO-LDFA 300 K).

reveals that electronic effects are clearly predominant for the H/W(100) case, whereas coupling to lattice vibrations is the main channel of energy loss for N/W(100). Same conclusions have been drawn by Novko *et al* in their studies of H/Pd(100) and N/Ag(111) systems[79,80].

The high sticking probability (close to 1) obtained for this energy range has been observed in other theoretical simulations making use of different PES and different methodologies. Recent theoretical works[41] exhibits the same trend with a uniformly high sticking probability close to unity for H on Ni(111). A slight decrease of the probability from ∼1 to ∼0.6 is only observed at very high collision energy (> 3 eV).

In Fig. 4, a decomposition of the sticking probability in two mechanisms is proposed for a larger collision energy range going from 10 meV to 5 eV. In this work we will define as low energy regime all collision energies between 10 meV and 1 eV. High energy regime belongs to collision energies higher than 1 eV. The first mechanism corresponds to adsorption of the atom on the surface. The second mechanism is associated to an absorption of the atom between the first and the third layer of the slab. Atoms that reaches the third layer with velocity vector pointing towards the bulk are also counted as absorbed.

For both H,N/W(100) the sticking probability is mainly due to atoms adsorbed on the surface at the low energy regime. As expected from the analysis of the PES, H atoms are able to penetrate into the bulk and being absorbed. The absorption process is rather independent of the H collision energy and represents about 10% of probability. By increasing collision energy beyond 1 eV, the sticking probability is decreasing with adsorption probability leading to more reflections, whereas absorption is slightly increasing from 10 to 20%. The N/W(100) dynamics are much simpler since only adsorption onto the surface is observed, the adsorption probability only slightly decreasing with energy. No absorption is observed even if initial collision energy is high enough to penetrate into the bulk and overcome the 2 eV barrier observed along the bridge site.

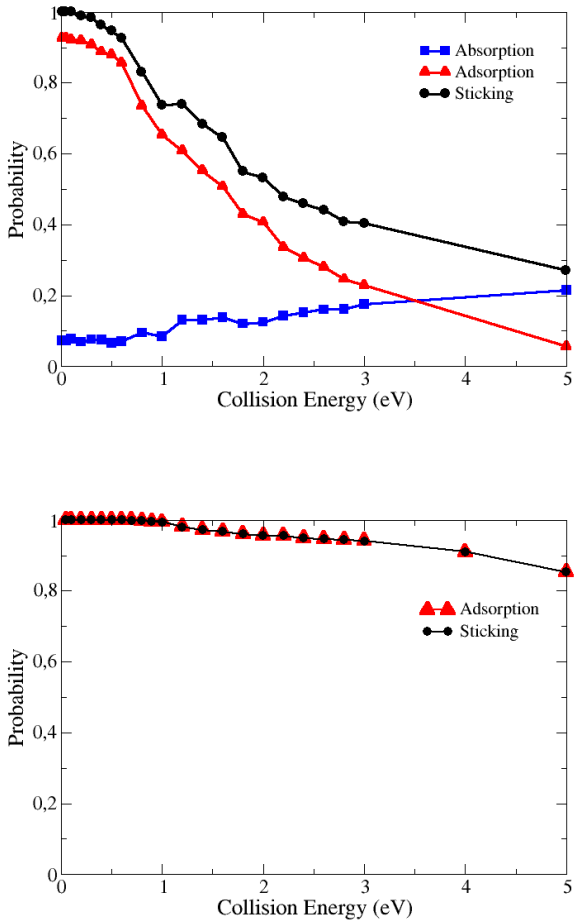

FIG. 4. Decomposition of the sticking probabilities in adsorption and absorption probabilities for H/W(100) (upper panel) and N/W(100) (lower panel) within the GLO-LDFA model at 300K.

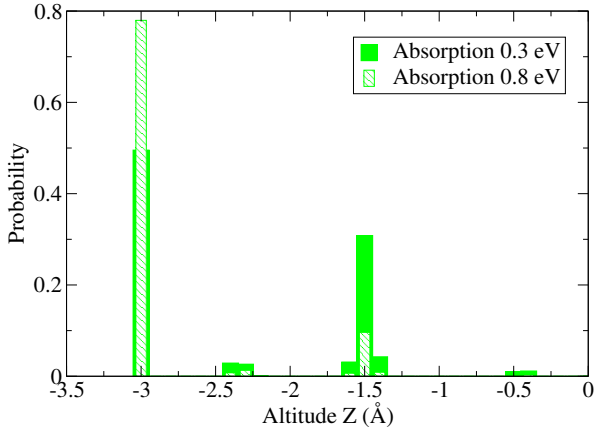

FIG. 5. Distribution of final altitudes for H-atoms absorbed into the bulk at 0.3 and 0.8 eV of collision energy. Simulations are done within the GLO-LDFA model with a surface temperature of 300K. The histogram at Z=−3.0 Å is not reflecting trajectories absorbed on a localized absorption site but rather hot atoms moving towards lower values of Z and penetrating into the bulk

Insights into the Adsorption and Absorption Processes

Within the low energy regime, an analysis of the final Z distribution of the absorbed H atoms reveals three sites of absorption below the top layer (see Fig. 5 where Z-distributions are plotted for 0.3 eV and 0.8 eV of initial collision energies). A detailed analysis allow us to locate those absorption sites on bridge site for the $Z = -0.40$ and -2.37 Å distances, and on top-to-bridge (T2B) site for $Z = -1.55$ Å.

Those 3 sites of absorption are thus populated at both 0.3 and 0.8 eV, for trajectories initiated with normal incidence to the surface. The most populated site is the T2B, especially at 0.8 eV, even if it is not the site characterized by the highest binding energy (see Table 1 for a comparison of the binding energy over the 3 adsorption sites). A non negligible proportion of the adsorbed atoms scatters into the bulk, as revealed by the histograms at Z=−3.0 Å, which altitude corresponds to the lowest altitude trajectories can reach in the simulations. In Table 1, mean energy losses are compared for trajectories ending into absorption sites, with an initial total energy of 0.3 eV. The mean energy loss which corresponds to those trajectories still in scattering is rather small (0.73 eV) leading to "hot atoms" characterized by mean total energy of about -0.43 eV, that is enough to overcome all the barriers to travel through the three first layers of the slab as can be seen on Fig. 6, where the potential energy as a function of the scattering path is depicted. The high energy regime is characterized by absorbed species still scattering into the bulk and none of them remains trapped into one of the 3 absorption sites identified at lower energies.

The scattering pathway into the bulk observed in the simulations is the Bridge-T2B-Bridge, as depicted in the Fig. 6. In short, the atoms that are neither reflected nor adsorbed penetrate the surface through the Bridge site and find the absorption site 1 (Bridge-1) and then migrate to site 2 (T2B) overcoming a barrier of 0.73 eV. The site 2 is the most populated for absorption, as mentioned above. Then, the H-atoms undergoes a migration to the site 3 (Bridge-3), with an activation barrier of 0.28 eV. Sites 1, 2, 3 shown in Fig. 7 correspond to tetrahedral interstitial sites (TIS), so we have found that motion of H-atoms into the bulk occurs along a TIS−TIS−TIS path as exhibited in Fig. 8 where (X, Y)-positions of the atoms scattering into the bulk are plotted for different Z altitudes. As can be seen in the figure, trajectories first concentrate around the TIS-bridge site when reaching the altitude corresponding to the site 1, then atomic positions spread out from bridge to TIS-T2B at altitude belonging to site 2. Finally, atoms end on TIS-bridge po-

sitions at the altitude of the site 3. Similar results have been reported by Liu *et al*[81]. In the present work, it was also found that atoms absorbed in any of the three sites can remain trapped. The lack of kinetic energy does not allow them to move out of their absorption site.

Interestingly, absorbed atoms are weakly bounded when compared to species adsorbed on the surface (E_{bind}= 3.08 eV), which makes this system a promising candidate for sub-surface recombination reactions with atoms coming from the gas phase. Results reported by Markejl *et al*[82] suggests there must be another recombination mechanism apart from Eley-Rideal surface recombination. Such a mechanism is characterized by a large exothermicity (of about 4 eV), producing vibrationally hot molecules. Exothermicity of Eley-Rideal path can not explain the highly hot molecules they observe. In our work, if one consider sub-surface recombination, with most of the exothermicity transferred to vibration motion, one could expect producing molecules excited until $v = 7$ vibrational state. Further simulation work would be required to study in details such sub-surface reactions.

As expected, the adsorption mechanism leads to H-atoms adsorbed on bridge site, whereas hollow site characterizes the adsorption of N-atoms. Reflection is a fast process decided rather quickly in less than two rebounds (a rebound is defined here as a sign change in the Z linear momentum), whereas adsorption mechanism (with 60 rebounds in average) and absorption (90 rebounds) mechanisms are characterized by a large number of rebounds. The "hot" absorbed atoms still scattering into the bulk follow a rather direct mechanism with a relatively small number of rebounds (around 10 rebounds) explaining the weak loss of energy experienced by the atoms in the latter case. Same kind of conclusions has been drawn for the N/W(100) with a fast direct reflection mechanism and an indirect mechanism of adsorption mediated through trapping and energy dissipation (around 30 rebounds).

The distribution of minimum distance reached by the atoms being either reflected, or adsorbed are represented on Fig. 9. As previously identified for H scattering on Au[37,38], the atomic adsorption follows a penetration/resurfacing mechanism for both H/W(100) and N/W(100). If we consider penetration to happen when the atom goes below $Z = 0$, roughly 60% of the H atoms adsorbed on W(100) has followed a penetration/resurfacing mechanism, against 15% for the N atoms case. In comparison, for H on Au(111) Janke *et al.*[38] found a penetration-resurfacing contribution of about 80% at 2.7 eV of incidence energy. At 0.8 eV, H-atoms can penetrate as deep as Z=−2 Å before resurfacing and being adsorbed on a bridge site of the surface. The loss of energy by electronic friction is enhanced by this penetration effect. For N-atoms, the penetration is somehow weaker since Z=−0.5 Å is only rarely reached at low collision energies. N/W(100) PES does not allow penetration of the atoms as easily as in the H-atoms case, and loss of

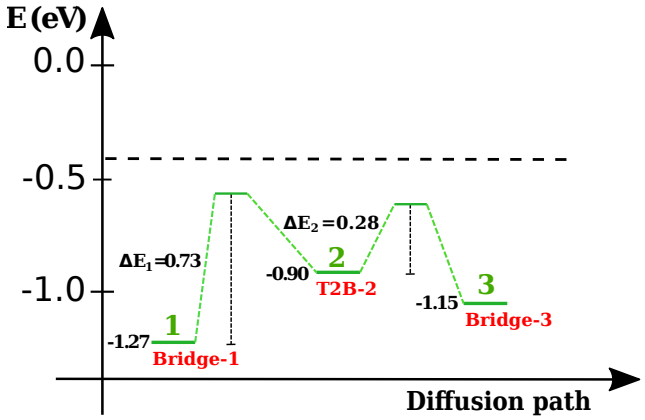

FIG. 6. Energetic scheme of the H-atoms in motion throughout the W(100) slab following the TIS-TIS-TIS pathway. Dashed line corresponds to the mean total energy of atoms reaching the -3.0 Å limit with a 0.3 eV of initial collision energy.

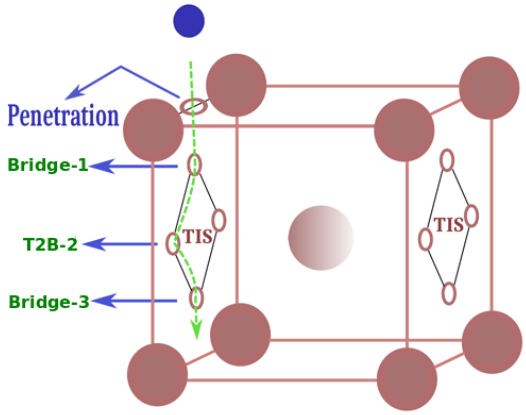

FIG. 7. Representation of the TIS-TIS-TIS pathway along sites 1, 2, and 3 within the W bcc unit cell. Projected onto (100) plane, site 1 corresponds to a bridge site, site 2 to a T2B site, and site 3 to a bridge.

Energy (eV)	Absorption sites, Z(Å)		
	−0.40	−1.55	−2.33
$\langle E_{loss} \rangle$	1.56	1.19	1.40
E_{bind}	1.27	0.90	1.15

TABLE I. Analysis of energy for absorption sites. The initial collision energy is 0.3 eV.

energy through coupling with the surface atoms motion is preventing any absorption even at energies higher than 2 eV (lowest energy barrier for absorption through the bridge site). In order to check this point, BOSS trajectories calculations have been performed for the N/W system. Within the BOSS approximation, where no energy exchange is allowed, all atoms approaching the surface at the vicinity of the bridge site with energies higher than 2 eV penetrate into the bulk reaching the Z=−3.0 Å limit.

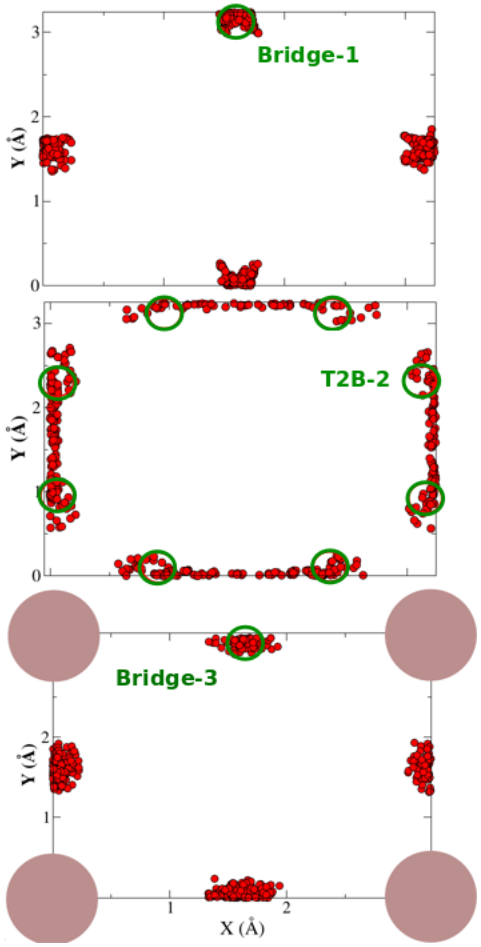

FIG. 8. X and Y distributions of atoms scattering into the bulk displayed for different values of Z that correspond to altitudes of site 1 (Z=-0.4 Å, upper panel), site 2 (Z=-1.55 Å, center panel), and site 3 (Z=-2.33 Å, lower panel).

As soon as GLO model is used in the simulations no more absorption is observed for the same conditions, exhibiting the strong influence of this energy loss channel. We have checked that the Z-limit used in the dynamics (Z=−3.0 Å) is low enough not to have any influence on the adsorption probability and the resurfacing mechanism.

Energy loss upon H reflection on W(100)

For several (111) *fcc* metal surfaces (i.e. Au, Pt, Ag, Pd, Cu, and Ni), comparison between theoretical simulations and atomic beam experiments has been performed[41] by considering energy loss spectra for H-atoms scattering back to the vacuum. In this work, H-atoms inelastic scattering has been analyzed for a high collision energy of 1.92 eV and off-normal incidence (initial angle of the beam with respect to the surface normal vector equal to 45°). It was found that the average energy loss is about 0.75 eV and very similar for all metals ranging from the lightest (Ni) to the heaviest surface

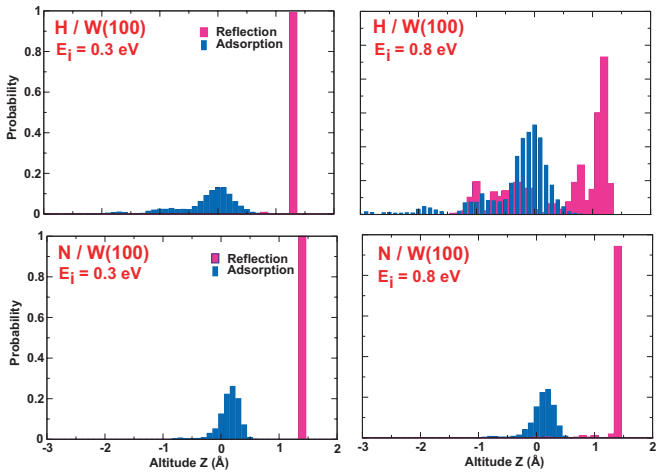

FIG. 9. Distributions of minimum altitudes reached by H-atoms (upper panel) and N-atoms (lower panel) either reflected, or adsorbed on the surface for two different initial collision energies (E_i): 0.3 and 0.8 eV within the GLO-LDFA model at 300K.

atoms (Au). Because the loss of energy is mainly due to electronic effects (that depend only weakly on the metal under study when compared to surface motion dissipation channel, where the mass is playing a key role), there is no significant change with the nature of the metal.

For comparison, the energy loss spectra of H scattering off the W(100) surface has been displayed in Fig. 10, for an initial energy of 1.92 eV and two incidence angles (normal incidence and off normal incidence with a polar angle of 45° taking an average over all azimuthal angles). In the off-normal case the mean energy loss is 0.8 eV in close agreement with previous work[41] on other metals. The shape of the energy loss spectrum exhibits three peaks, that can be attributed to reflections at different values of Z, roughly 1.2, -0.5, and -2 Å. As expected, the highest is the penetration of the atoms (i.e. the lowest altitude), the highest is the energy loss by electronic friction since atoms then travel in regions where electronic density is high. As a consequence, the third peak between 1.0 and 1.5 eV of energy loss is attributed to the reflection at lowest altitude i.e. $Z = -2$ Å. A comparison between normal and off-normal curves tends to show that incidence barely affect the energy loss. We also checked that sticking probability is weakly influenced by the incidence angle (calculations were made from normal incidence to 75° off-normal incidence). As a matter of fact the penetration to subsurface area is not influenced so much by the incidence angle since it often happens after long residence time at the vicinity of the surface where trapping mechanism dominates involving a significant loss of memory. The energy dissipation to the electrons of the surface follows total energy scaling (TES) process whatever if considering reflection, or sticking.

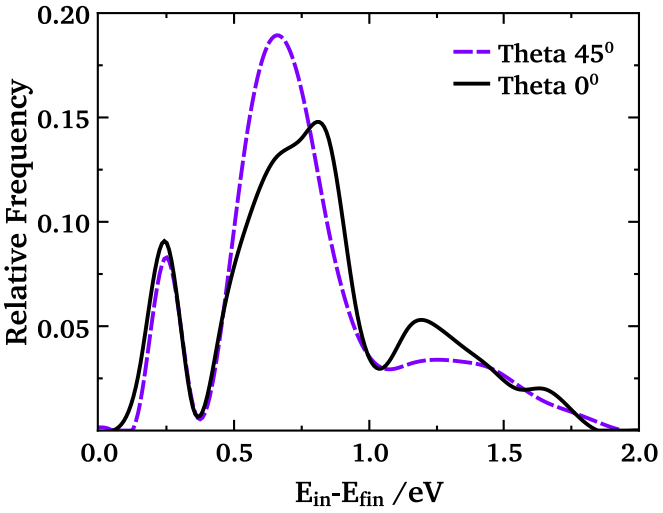

FIG. 10. Total energy loss spectra (in eV) of reflected atoms for an initial collision energy of 1.92 eV. Two values of incidence angles are reported (normal incidence and off normal incidence with a polar angle of 45 degrees averaged over all azimuthal angles). The distributions are normalized to the area. GLO-LDFA model.

IV. SUMMARY AND REMARKS

Scattering dynamics of H and N atoms on W(100) has been investigated by means of theoretical simulations. A special focus has been made on sticking mechanism discriminated into adsorption and absorption processes. As also demonstrated elsewhere[33,36–42], the H-atoms sticking is mediated through energy dissipation to electrons whereas coupling to lattice vibrations plays the major role for the case of N-atoms. H-atoms can penetrate the W slab through the bridge sites and either end absorbed on various sub-surface sites (bridge and T2B) between topmost and third layer, or scatter as hot atoms deeper into the bulk. The H-atoms motion between the top layer and the third layer of the slab occurs following a TIS−TIS−TIS path way. Part of the H-atoms adsorption mechanism follows the so-called penetration/resurfacing scheme already proposed in early works.[37] Sub-surface adsorbed H-atoms have been characterized and could potentially lead to recombination events with atoms coming from the gas phase, producing highly vibrationally excited molecules. Further theoretical works would be required to confirm this possible scenario.

Within the energy range considered in the simulations, the sticking of N-atoms is only described through the adsorption. No absorption is observed as the N/W(100) dynamics, strongly influenced by the loss of energy through lattice motion, prevents any penetration below -1.5 Å. For both H and N atoms the reflection is a direct process whereas sticking is characterized by indirect mechanisms involving many rebounds before the atoms remain thermalized on the surface. The energy loss spectra of the reflected back H-atoms has been studied, exhibiting total energy scaling behavior. The mean energy loss determined in our simulations is in close agreement with previous experimental and theoretical works on H scattering on several *fcc* metal (111) surfaces (Ni, Cu, Pd, Ag, Au, Pt). Therefore, our theoretical predictions for a (100) surface of a *bcc* metal reinforce this general feature of the electronically nonadiabatic adsorption process of atomic H on metals[37]. Further studies would be required to fully understand the features of the energy loss spectra in relation with surface structure and symmetry.

Acknowledgments

This work was conducted in the scope of the transborder joint Laboratory QuantumChemPhys: Theoreti- cal Chemistry and Physics at the Quantum Scale (ANR-10- IDEX-03-02).Computer time was provided by the Pole Modelisation computing facilities of the Institut des Sciences Moleculaires (UMR5255, CNRS/U. Bordeaux), partly funded by the Nouvelle Aquitaine Region

[1] I. Langmuir, *J. Am. Chem. Soc.*, 1912, **34**(10), 1310–1325.
[2] M. Andersson, F. Abild-Pedersen, I. Remediakis, T. Bligaard, G. Jones, J. Engbæk, O. Lytken, S. Horch, J. Nielsen, J. Sehested, J. Rostrup-Nielsen, J. Nørskov, and I. Chorkendorff, *J. Catal.*, 2008, **255**(1), 6 – 19.
[3] A. Nilsson, L. G. M. Petersson, , and J. K. Nørskov, *Chemical Bonding at Surface and Interfaces*, Elsevier, Amsterdam, 2008.
[4] G. A. Somorjai, *Introduction to Surface Chemistry and Catalysis*, Wiley, New York, 1994.
[5] I. Chorkendorff and J. W. Niemantsverdriet, *Concepts of Modern Catalysis and Kinetics*, Wiley-VCH, Weinheim, 2003.
[6] G. Ertl, *J. Vac. Sci. Technol. A*, 1983, **1**, 1247.
[7] K. Honkala, A. Hellman, I. N. Remediakis, A. Logadottir, A. Carlsson, S. Dahl, C. H. Cristensen, and J. K. Nørskov, *Science*, 2005, **307**, 55.
[8] I. Takagi, S. Nomura, T. Minamimoto, M. Akiyoshi, T. Kobayashi, and T. Sasaki, *J. Nucl. Mat.*, 2015, **463**, 1125 – 1128.
[9] K. Heinola, T. Ahlgren, K. Nordlund, and J. Keinonen, *Phys. Rev. B.*, 2010, **82**, 094102.
[10] D. Terentyev, V. Dubinko, A. Bakaev, Y. Zayachuk, W. V. Renterghem, and P. Grigorev, *Nucl. Fusion*, 2014, **54**(4), 042004.
[11] H.-B. Zhou, Y.-L. Liu, S. Jin, Y. Zhang, G. Luo, and G.-H. Lu, *Nucl. Fussion*, 2010, **50**(2), 025016.
[12] M. Capitteli, *NATO ASI Ser., C, Kluwer Academic Publishers Dordrecht*, 1989, **482**.
[13] M. Cacciatore, M. Rutigliano, and G. D. Billing, *J. Thermophys Heat Transfer*, 1999, **13**, 195.
[14] D. Bruno, M. Cacciatore, S. Longo, and M. Rutgliano, *Chem. Phys. Lett.*, 2000, **320**, 245.
[15] L. Bedra, M. Rutigliano, M. Balat-Pichelin, and M. Cacciatore, *Langmuir*, 2006, **22**, 7208.
[16] M. Rutigliano, A. Pieretti, M. Cacciatore, N. Sanna, and V. Barone, *Surf. Sci.*, 2006, **600**, 4239.
[17] N. Perron, N. Pineau, E. Arquis, J. C. Rayez, and A. Salin, *Surf. Sci.*, 2005, **599**, 160.
[18] C. Arasa, P. Gamallo, and R. Sayos, *J. Phys. Chem. B.*, 2005, **109**, 14954.
[19] L. Bedra, M. J. H. Balat-Pichelin, M. Rutigliano, and M. Cacciatore, *AIP Conf. Proc.*, 2005, **762**, 1037.
[20] E. J. Jumper and W. A. Seward, *J. Thermophys. Heat Transfer*, 1991, **5**, 284.
[21] R. J. Willey, *J. Thermophys. Heat Transfer*, 1993, **7**, 55.
[22] O. Deutschmann, U. Riedel, and J. Warnatz, *J. Heat Transfer*, 1995, **117**, 495.

[23]S. Reggiani, M. Barbato, C. Bruno, and J. Muylaert, *J. Thermophys. Heat Transfer*, 2000, **14**, 412.
[24]T. Kurotaki, *AIAA paper*, 2000, p. 2366.
[25]B. Halpern and D. E. Rosner, *J. Chem. Soc., Faraday Trans.*, 1978, **74**, 1883.
[26]B. van Ootegem, D. Conte, N. Sauvage, P. Tran, P. Vervisch, A. Desportes, P. Regnier, C. Crespos, P. Larregaray, J. C. Rayez, E. Arquis, and N. Perron, *4th International Symposium on Atmospheric Vehicles and Systems*.
[27]M. Balat-Pichelin, M. Czerniak, and J. M. Badie, *J. Spacecr. Rockets*, 1999, **36**, 273.
[28]M. Balat-Pichelin, M. Czerniak, and J. M. Badie, *Appl. Surf. Sci.*, 1997, **120**, 225.
[29]V. Moron, P. Gamallo, L. Martin-Gondre, C. Crespos, P. Larregaray, and R. Sayos, *Phys. Chem. Chem. Phys.*, 2011, **13**, 17494.
[30]V. Moron, L. Martin-Gondre, C. Crespos, P. Larregaray, P. Gamallo, and R. Sayos, *Comp. Theo. Chem.*, 2012, **990**, 132.
[31]L. Martin-Gondre, M. Alducin, G. A. Bocan, R. Díez-Muiño, and J. I. Juaristi, *Phys. Rev. Lett.*, 2012, **108**(9), 096101.
[32]L. Martin-Gondre, G. A. Bocan, M. Alducin, J. I. Juaristi, and R. Díez-Muiño, *Comp. Theo. Chem.*, 2012, **990**, 126–131.
[33]M. Blanco-Rey, J. I. Juaristi, R. Díez Muiño, H. F. Busnengo, G. J. Kroes, and M. Alducin, *Phys. Rev. Lett.*, 2014, **112**, 103203.
[34]H. F. Busnengo, M. A. Di Césare, W. Dong, and A. Salin, *Phys. Rev. B*, 2005, **72**(12), 125411.
[35]J. I. Juaristi, M. Alducin, R. D. Muino, H. F. Busnengo, and A. Salin, *Phys. Rev. Lett.*, 2008, **100**, 116102.
[36]J. Nørskov and B. Lundqvist, *Surf. Sci.*, 1979, **89**(1), 251 – 261.
[37]O. Bünermann, H. Jiang, Y. Dorenkamp, A. Kandratsenka, S. M. Janke, D. J. Auerbach, and A. M. Wodtke, *Science*, 2015, **350**(6266), 1346–1349.
[38]S. M. Janke, D. J. Auerbach, A. M. Wodtke, and A. Kandratsenka, *J. Chem. Phys.*, 2015, **143**(12), 124708.
[39]M. Pavanello, D. J. Auerbach, A. M. Wodtke, M. Blanco-Rey, M. Alducin, and G.-J. Kroes, *J. Phys. Chem. Let*, 2013, **4**(21), 3735–3740.
[40]G.-J. Kroes, M. Pavanello, M. Blanco-Rey, M. Alducin, and D. J. Auerbach, *J. Chem. Phys.*, 2014, **141**(5), 054705.
[41]Y. Dorenkamp, H. Jiang, H. Köckert, N. Hertl, M. Kammler, S. M. Janke, A. Kandratsenka, A. M. Wodtke, and O. Bünermann, *J. Chem. Phys.*, 2018, **148**(3), 034706.
[42]M. A. Zeb, J. Kohanoff, D. Sánchez-Portal, A. Arnau, J. I. Juaristi, and E. Artacho, *Phys. Rev. Lett.*, 2012, **108**, 225504.
[43]R. Pitts, A. Kukushkin, A. Loarte, A. Martin, M. Merola, C. Kessel, V. Komarov, and M. Shimada, *Phys. Scr.*, 2009, **138**, 014001.
[44]N. Fernandez, Y. Ferro, and D. Kato, *Acta Mater.*, 2015, **94**, 307 – 318.
[45]Y. Liu, H. Z. Y. Zhang, F. L. G.H. Lu, and G. Luo, *Phys. Rev. B.*, 2009, **79**, 172103.
[46]K. Heinola and T. Ahlgren, *J. Appl. Phys.*, 2010, **107**, 113531.
[47]D. Johnson and E. Carter, *J. Mater. Res.*, 2010, **25**, 315.
[48]W. Shu, E. Wakai, and T. Yamanishi, *Nucl. Fusion*, 2007, **47**(3), 201.
[49]O. Galparsoro, R. Pétuya, H. Busnengo, J. Juaristi, C. Crespos, M. Alducin, and P. Larregaray, *Phys. Chem. Chem. Phys.*, 2016, **18**, 31378–31383.
[50]O. Galparsoro, H. F. Busnengo, A. E. Martinez, J. I. Juaristi, M. Alducin, and P. Larregaray, *Phys. Chem. Chem. Phys.*, 2018, **20**, 21334–21344.
[51]O. Galparsoro, R. Pétuya, J. Juaristi, C. Crespos, M. Alducin, and P. Larregaray, *J. Phys. Chem. C.*, 2015, **119**(27), 15434–15442.
[52]G. Volpilhac, H. F. Busnengo, W. Dong, and A. Salin, *Surf. Sci.*, 2003, **544**, 329–338.
[53]J. Strömquist, L. Bengtsson, M. Persson, and B. Hammer, *Surf. Sci.*, 1998, **397**(1), 382 – 394.
[54]W. Kohn and L. J. Sham, *Phys. Rev.*, 1965, **140**, A1133.
[55]P. Hohenberg and W. Kohn, *Phys. Rev.*, 1964, **136**, 864.
[56]K. Lee, E. D. Murray, L. Kong, B. I. Lundqvist, and D. C. Langreth, *Phys. Rev. B.*, 2010, **82**, 081101.
[57]A. Peña-Torres, H. F. Busnengo, J. I. Juaristi, P. Larregaray, and C. Crespos, *Phys. Chem. Chem. Phys.*, 2018, **20**(29), 19326–19331.
[58]A. Pena-Torres, H. F. Busnengo, J. I. Juaristi, P. Larregaray, and C. Crespos, *J. Phys. Chem. C.*, 2019, **123**(5), 2900–2910.
[59]D. Migliorini, F. Nattino, and G.-J. Kroes, *J. Chem. Phys.*, 2016, **144**(8), 084702.
[60]L. Martin-Gondre, J. I. Juaristi, M. Blanco-Rey, R. D. Muiño, and M. Alducin, *J. Chem. Phys.*, 2015, **142**(7), 074704.
[61]H. F. Busnengo, A. Salin, and W. Dong, *J. Chem. Phys.*, 2000, **112**(17), 7641–7651.
[62]R. A. Olsen, H. F. Busnengo, A. Salin, M. F. Somers, G. J. Kroes, and E. J. Baerends, *J. Chem. Phys.*, 2002, **116**, 3841.
[63]G. Kresse, *Phys. Rev. B.*, 2000, **62**, 8295.
[64]A. D. Becke, *Phys. Rev. A*, 1988, **38**, 3098.
[65]J. P. Perdew, *Phys. Rev. B*, 1986, **33**, 8822.
[66]D. Vanderbilt, *Phys. Rev. B (Rapid Communication)*, 1990, **41**, 7892.
[67]K. Laasonen, R. Car, C. Lee, and D. Vanderbilt, *Phys. Rev. B (Rapid Communication)*, 1991, **43**, 6796.
[68]K. Laasonen, A. Pasquarello, C. Lee, R. Car, and D. Vanderbilt, *Phys. Rev. B*, 1993, **47**, 10142.
[69]J. Hafner and G. Kresse, in *Properties of Complex Inorganic Solids*, ed. A. Gonis, A. Meike, and P. E. A. Turchi, Springer US, Boston, MA, 1997; pp. 69–82.
[70]G. Kresse and J. Hafner, *Phys. Rev. B.*, 1993, **47**, 558.
[71]G. Kresse and J. Hafner, *Phys. Rev. B.*, 1993, **48**, 13115.
[72]G. Kresse and J. Furthmuller, *Comput. Mater. Sci.*, 1996, **6**, 15.
[73]G. Kresse and J. Furthmuller, *Phys. Rev. B.*, 1996, **54**, 11169.
[74]F. Nattino, O. Galparsoro, F. Costanzo, R. Diez Muino, M. Alducin, and G. Kroes, *J. Chem. Phys.*, 2016, **144**, 244708.
[75]H. F. Busnengo and A. E. Martinez, *J. Phys. Chem. C*, 2008, **112**, 5579–5588.
[76]M. R. Barnes and R. F. Willis, *Phys. Rev. Lett.*, 1978, **41**(25), 1729–1733.
[77]P. Alnot, A. Cassuto, and D. A. King, *Surf. Sci.*, 1989, **215**, 29–46.
[78]C. Ibarguen, P. Larregaray, A. Peña-Torres, and C. Crespos, *J. Phys. Chem. C*, 2018, **122**(50), 28856–28861.
[79]D. Novko, M. Blanco-Rey, J. I. Juaristi, and M. Alducin, *Phys. Rev. B*, 2015, **92**, 201411.
[80]D. Novko, M. Blanco-Rey, J. I. Juaristi, , and M. Alducin, *Phys. Rev. B*, 2016, **93**, 245435.
[81]Y.-N. Liu, T. Wu, Y. Yu, X.-C. Li, X. Shu, and G.-H. Lu, *J. Nucl. Mater.*, 2014, **455**(1-3), 676–680.
[82]S. Markelj and I. Cadez, *J. Chem. Phys.*, 2011, **134**, 124707.

Highlights

- Scattering dynamics of light and heavy benchmark atoms on metal surface.
- Sticking mechanisms through various mechanisms : surface adsorption and absorption under penetration into sub-surface layers.
- Study of atom energy loss through lattice vibrations and electron-hole pairs excitation of the metal.

Atomic scattering of H and N on W(100): effect of lattice vibration and electronic excitations on the dynamics

C. Ibarguen Becerra,[1,2] C. Crespos,[1,2,a)] O. Galparsoro,[3,4] and P. Larregaray[1,2]
[1)] *Université Bordeaux, ISM, UMR5255, F-33400 Talence, France*
[2)] *CNRS, ISM, UMR5255, F-33400 Talence, France*
[3)] *Institute for Physical Chemistry , Georg-August University of Göttingen, Tammannstr. 6, 37077 Göttingen, Germany*
[4)] *Department of Dynamics at Surfaces, Max-Planck Institute for Biophysical Chemistry, Am Faßberg 11, 37077 Göttingen, Germany*

(Dated: 12 June 2020)

Scattering of H and N atoms from W(100) surface has been theoretically studied by means of classical trajectories based on an electronically adiabatic potential energy surface (PES). The PES has been constructed by interpolation of density functional theory (DFT) calculations following a corrugation reducing procedure (CRP). Van der Waals interactions are taken into account by using the vdW-DF2 exchange- correlation functional. In the dynamics a special focus is made on the influence of energy release through surface atoms motion and electrons of the metal. Most part of the H-atoms sticking is mediated through penetration into the sub-surface area where electron-hole pairs excitation plays the major role. For N-atoms the sticking is mainly due to the coupling with lattice vibrations, as expected when considering heavy atoms. Adsorption and absorption processes have been characterized for both H/W(100) and N/W(100) exhibiting differences between those benchmark light and heavy atoms in interaction with metals.

Keywords: Dynamics of atomic scattering on surfaces, theoretical simulations, quasi-classical trajectories, van der Waals forces.

I. INTRODUCTION

The scattering of atomic species on metal surfaces is of high interest in many domains of fundamental and applied science as for example heterogeneous catalysis[1–7], plasma-wall interactions in nuclear physics[8–11], or for the aerothermochemistry of thermal protection systems in atmospheric reentries[12–30]. A key question to address is the release of energy into the surface by means of coupling between the translational degrees of freedom of the atom and the surface atoms motion or the electrons of the solid[31–35]. H-atom sticking, after single or multiple collisions with the surface, has been shown to occur mainly through loss of energy due to electron-hole (e-h) pairs excitations[33,36–42]. Because of the large mass mismatch between atoms of the metal and hydrogen, transfer of energy to the lattice vibrations is unlikely to occur. Recent experimental and theoretical works on H-atom collision with several (111) surfaces of *fcc* transition metals (Au, Pt, Ag, Pd, Cu, and Ni) have exhibited a universal behavior with respect to nonadiabatic adsorption processes[41]. In this work, authors have shown that energy loss is almost independent of the metal and is mainly due to electronic friction. Since no influence of metals work functions is observed, authors also conclude that no charge transfer occurs between the impinging atom and the surface upon collision for an initial energy of 1.92 eV.

In this work, simulations have been performed on the H/W(100) benchmark system leading to a further analysis of the universal energy loss scheme proposed by Dorenkamp *et al.* in the context of a more open surface and a *bcc* metal. Moreover, the penetration of atomic hydrogen on W metal is of high interest in the context of nuclear physics[43–47]. As a matter of fact, the study of H scattering in tungsten has gained a lot of interest in the last decades in the context of plasma facing materials (PFMs)[43–47], in which tungsten is a promising candidate. Hydrogen is known to induce blisters formation when tungsten is exposed to the high flux plasma irradiation, specially at low incident energy.[48] It is also known that blistering problem induced by H retention may cause reduction of the lifetime of the material. Consequently, a discussion of first step H absorption and scattering into the solid is proposed, pointing out the importance of electronic friction for the description of sub-surface atoms motion.

For heavier atoms, such as nitrogen, energy exchange with lattice vibration are expected to be much more efficient. Scattering dynamics simulations are here also performed for N/W(100). Again, energy dissipation channels are included in the simulations addressing the question of the competition between both e-h pairs and lattice vibration excitation upon heavy atoms sticking on a metal surface[49–51]. Coupling between the normal and parallel motion of the N atoms mediated through corrugation has been shown to play a role[52,53] especially at low collision energy. A special focus on this issue is made in this work, by revisiting the early work of G. Volpilhac *et al.*[52,53] where no energy loss channels were included in the simulations.

A new potential energy surface (PES) has been built for H/W(100) by interpolation of density func-

[a)] cedric.crespos@u-bordeaux.fr

tional theory (DFT)[54,55] calculations making use of the vdW-DF2[56] exchange correlation functional. For the N/W(100), we have used a similar PES, developed and presented elsewhere[57,58]. The choice of the functional was originally motivated by previous works suggesting that dispersion forces may play an important role in the dynamics of molecules in interaction with metal surfaces[57–60]. However, comparing the vdW-DF2 based PESs with older ones calculated at PW91 level, no significant differences has been noticed for the particular cases of both N/W(100) and H/W(100). We have checked that the dynamics is almost unaltered by the choice of the functional in the energy range we consider in this work.

The paper is organized as follows: In Section II the computational details and methodology are presented. Results are discussed in Section III and a summary with the main conclusions is given in Section IV.

II. COMPUTATIONAL DETAILS

The interaction between H and N atoms with the W(100) surface has been modelled by a 3-dimensional PES which depends on X, Y, and Z coordinates referring the position of the H/N atom with respect to one surface atom at the origin of the Cartesian frame. The X and Y are along the sides of the square unit cell. In order to get a continuous 3D-PES a Corrugation reducing procedure (CRP)[61–63] has been used to interpolate a set of about 900 DFT single point calculations. A grid of 60 Z values above 15 sites of the surface have been sampled (see Fig. 1 for details).

A periodic supercell approximation has been used. The metallic surface is represented by a 5-layer slab, and the calculations were performed using a 15x15x1 Monkhorst-Pack grid of k points for a (2x2) structure. We obtained a bulk lattice constant of $a = 3.239$ Å. After relaxation, an interlayer distance of $0.437a$ has been found for the two topmost layers and of $0.517a$ between the second and the third layer. Spin-polarized DFT calculations have been carried out within the Generalized Gradient Approximation (GGA)[64,65] making use of the vdW-DF2[56] exchange-correlation functional. Ultrasoft pseudo-potentials[66–68] have been used to describe the interaction with atomic cores. All the calculations were performed with the Vienna Ab Initio Simulation Package (VASP)[69–73]. The 3-dimensional PES for H/W(100) has been built in the framework of this investigation, while the N/W(100) PES has been taken from the work of A. Pena-Torres et *al*[57].

The dynamics simulations are based on the adiabatic 3D-PESs making use of the classical trajectories method. In order to calculate probabilities for the different exit channels such as adsorption, absorption and/or reflection, 10000 trajectories have been performed for several initial collision energies ranging from 10 meV to 5.0 eV. The initial X and Y positions of the atoms above the W(100) unit cell were randomly selected leading to uniform sampling. All trajectories have been started at

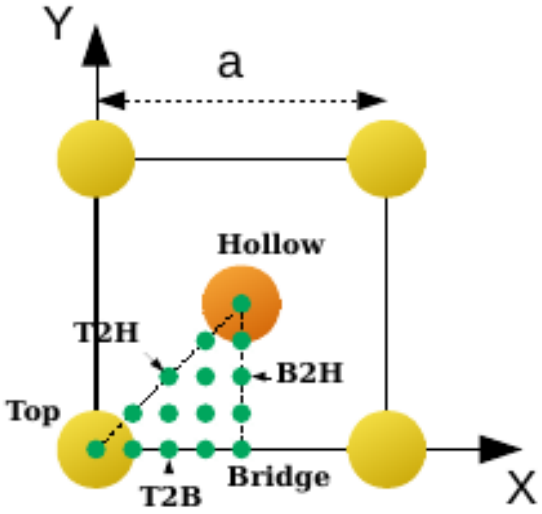

FIG. 1. Top-view of the unit cell and the sites (green points) for which DFT calculations have been carried out. W atoms in the first layer are in yellow. In orange W atom belongs to the second layer. Top, Bridge, Hollow, Top-to-Bridge (T2B), Top-to-Hollow (T2H), and Bridge-to-Hollow (B2H) high symmetry sites are shown. The lattice constant is $a = 3.239$ Å.

$Z_0 = 6.0$ and $Z_0 = 7.0$ Å from the surface in the asymptotic region of the PES for H and N atoms, respectively. Normal and off-normal incidence conditions have been analyzed. An atom is considered as reflected whenever it reaches back its initial distance from the surface Z_0 with a velocity pointing towards vacuum. Absorption occurs when atoms reach the value of $Z_{min} = -3.0$ Å which corresponds to a position slightly above the third layer of the slab. The atoms are also considered as absorbed if, after the maximum integration time of 2.0 ps, they remain between the top layer ($Z = 0$) and the third layer ($Z_{min} = -3.0$ Å) with kinetic energy lower than the one required to escape from the bulk. Adsorption occurs when the atom is neither reflected nor absorbed with a kinetic energy lower than the minimum required to escape the attractive potential of the surface. The maximum integration time of 2.0 ps has been chosen such that the exit channel probabilities are all converged.

In the calculations, a surface oscillator was used to simulate energy exchange between the atom and vibrations of the lattice via the so-called generalized Langevin oscillator (GLO) model[34]. Individual motions of surface atoms are not treated explicitly within the GLO model, thus lattice motion effects are accounted for in a very approximate way. Theoretical simulations performed by F. Nattino et al.[74] on N_2/W(110) system, have shown that despite its simplicity, the GLO model is able to capture the physics of the problem. For instance, N_2 dissociation probability on W(110) calculated at GLO level compares well with probability evaluated through more elaborated treatment such as Ab Initio Molecular Dynamics (AIMD) method. Moreover, those two methods predict very sim-

ilar energy transfer between the molecule and the lattice degrees of freedom for the case of non-reactive scattering events. Then energy dissipation to the metal mediated by e-h pairs excitations is modelled by an effective friction term introduced in the classical equations of motion, and evaluated through the Local density friction approximation (LDFA)[35,51]. Previous works on H scattering on various metals have excluded any formation of a transient H^- specie since energy loss spectra have been shown to be mostly independent of the work function of metals[41]. Thus, electronic excitations only treated at the LDFA level are expected to quantify correctly the energy loss of the atoms in interaction with the surface electron density.

III. RESULTS AND DISCUSSION

Analysis of the PES

In order to describe the main features of the PESs for the two systems under study, i.e., H/W(100) and N/W(100), 1D cuts of the potentials for the highest symmetry surface sites as a function of altitude Z are displayed in Fig. 2.

H/W(100)

In agreement with previous experimental and theoretical works[75–77], the bridge site is the most stable site for H adsorption on W(100) at $Z = 1.11$ Å with a 3.08 eV binding energy. The penetration of the H atom into the slab is energetically favorable through the bridge site with barriers below the asymptotic potential energy. At large distances (between 2.0 and 3.0 Å) the top site is the most attractive site. On Fig. 2, three sites of absorption have been identified and labeled as 1, 2, and 3. We have checked that each of those sites corresponds to true minima of the 3D-PES by visualizing 2D-cuts as a function of X and Y coordinates for the different Z values of the 3 sites.

N/W(100)

For N/W, the most stable site is the hollow at $Z = 0.63$ Å with a 6.75 eV binding energy, rather similar to that of the B2H site, in agreement with previous results reported for Volpilhac et *al*[52]. The absorption process is shown to be activated with a barrier height of about 2 eV on the bridge (with respect to the origin of the potential energy that is set for N far from the surface), whereas the top site remains as the most attractive site at large distances, like in the H/W case.

For both H/W and N/W a comparison with previous PESs based on PW91 functional has been made and, in contrast to what was found for N_2,[57,78] for instance, no significant changes have been noticed by adding van der Waals contributions to the description of atom-surface interaction. This result may be due to the rather weak polarizability of the H and N atoms.

Sticking Probability

The total sticking probability S_0, defined as $S_0 = 1 - P_{ref}$ with P_{ref} being the atomic reflection probability, is plotted in Fig. 3 as a function of initial collision energy (E_i). Results for both H and N + W(100) are included. A comparison is made between the sticking probabilities calculated using three models previously described: (i) the static surface approximation (Born-Oppenheimer static surface - BOSS) for which no exchange of energy is accounted for, (ii) the GLO model to allow energy dissipation to lattice vibrations and account for surface temperature (here 300K) (iii) the GLO-LDFA model in which both surface motion and *e-h* pairs excitations are accounted for in the simulations (GLO-LDFA). By comparing the three models, it is possible to infer which dissipation channel dominates energy transfer to the surface.

From the information contained in Fig. 3 arises that, within the BOSS model, the sticking probability of H decreases sharply when the initial collision energy increases to approximately 200 meV and then remains almost constant up to 1 eV. In the case of N/W, S_0 decreases monotonically throughout the range when energy is increased, as has been observed in earlier theoretical simulations,[52] where it has been shown that dynamic trapping governs the sticking of atoms at low energy. Within the BOSS level, only transfer of energy between the perpendicular and parallel motion of the atom can lead to trapped atoms. By increasing collision energy this transfer becomes rapidly inefficient and the sticking probability gets small. At this level of approximation, one may compare the present BOSS results with the ones obtained by Volpilhac *et al*[52] on a PW91 based PES, for collision energy going from 10 meV to 1 eV. In their study, absorption was supposed to occur whenever trajectories were able to reach the top surface layer located at $Z = 0$. Then, the calculation was stopped and those trajectories were accounted for in the sticking probability. For comparison purposes, we have performed a calculation of the sticking probability using the same criteria. An almost identical sticking curve is obtained with a sharp decrease and a plateau at about 0.5. If atoms are allowed to travel between $Z = -3.0$ and 0 Å in the simulations, the sticking probability is largely reduced (with a value of 0.1 for 1 eV of collision energy (see Fig. 3) and composed uniquely of long-lived species bouncing on the surface with high kinetic energy. This result shows that resurfacing[37] and sub-surface motion plays an important role in the dynamics and should be accounted for in the simulations.

Going beyond the BOSS model by including energy dissipation channels increases significantly the trapping of atoms within the energy range considered in Fig. 3 and previous studies of Volpilhac *et al.*[52], i.e., 10 meV $\leqslant E_i \leqslant$ 1 eV. A comparison of the GLO and GLO-LDFA curves

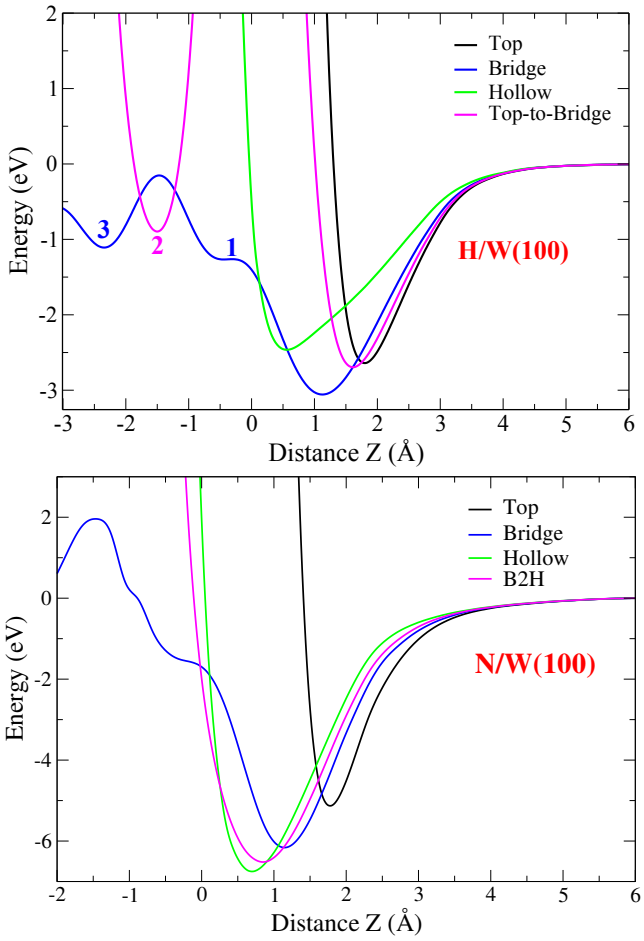

FIG. 2. 1D cuts of the potential energy surface as a function of atom/surface distance Z for several high symmetry sites. The upper panel corresponds to H/W(100) systems. 1, 2, 3 refers to absorption sites. The lower panel corresponds to N/W(100). Energies and distances are given in eV and Å, respectively.

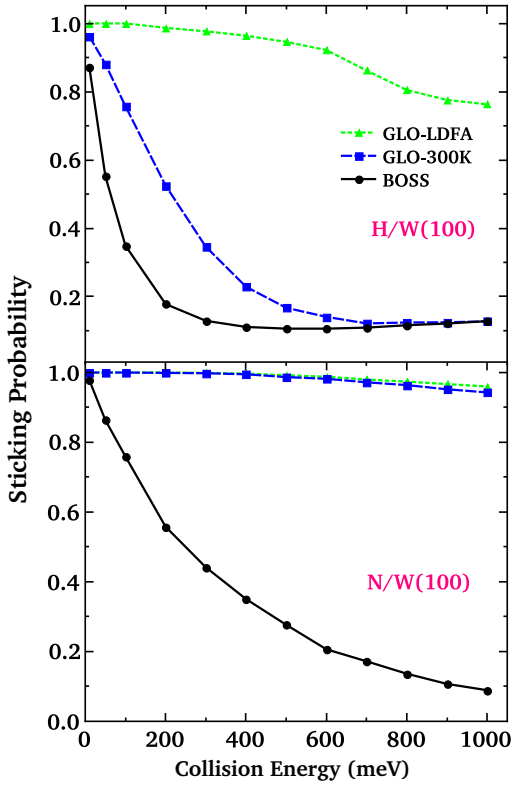

FIG. 3. Sticking probabilities as a function of atomic collision energy for H/W(100) (upper panel) and N/W(100) (lower panel). A comparison is made between simulations with no energy dissipation channels (BOSS), only phonons (GLO 300 K) and both phonons and electronic dissipation channels (GLO-LDFA 300 K).

reveals that electronic effects are clearly predominant for the H/W(100) case, whereas coupling to lattice vibrations is the main channel of energy loss for N/W(100). Same conclusions have been drawn by Novko *et al* in their studies of H/Pd(100) and N/Ag(111) systems[79,80].

The high sticking probability (close to 1) obtained for this energy range has been observed in other theoretical simulations making use of different PES and different methodologies. Recent theoretical works[41] exhibits the same trend with a uniformly high sticking probability close to unity for H on Ni(111). A slight decrease of the probability from ∼1 to ∼0.6 is only observed at very high collision energy (> 3 eV).

In Fig. 4, a decomposition of the sticking probability in two mechanisms is proposed for a larger collision energy range going from 10 meV to 5 eV. In this work we will define as low energy regime all collision energies between 10 meV and 1 eV. High energy regime belongs to collision energies higher than 1 eV. The first mechanism corresponds to adsorption of the atom on the surface. The second mechanism is associated to an absorption of the atom between the first and the third layer of the slab. Atoms that reaches the third layer with velocity vector pointing towards the bulk are also counted as absorbed.

For both H,N/W(100) the sticking probability is mainly due to atoms adsorbed on the surface at the low energy regime. As expected from the analysis of the PES, H atoms are able to penetrate into the bulk and being absorbed. The absorption process is rather independent of the H collision energy and represents about 10% of probability. By increasing collision energy beyond 1 eV, the sticking probability is decreasing with adsorption probability leading to more reflections, whereas absorption is slightly increasing from 10 to 20%. The N/W(100) dynamics are much simpler since only adsorption onto the surface is observed, the adsorption probability only slightly decreasing with energy. No absorption is observed even if initial collision energy is high enough to penetrate into the bulk and overcome the 2 eV barrier observed along the bridge site.

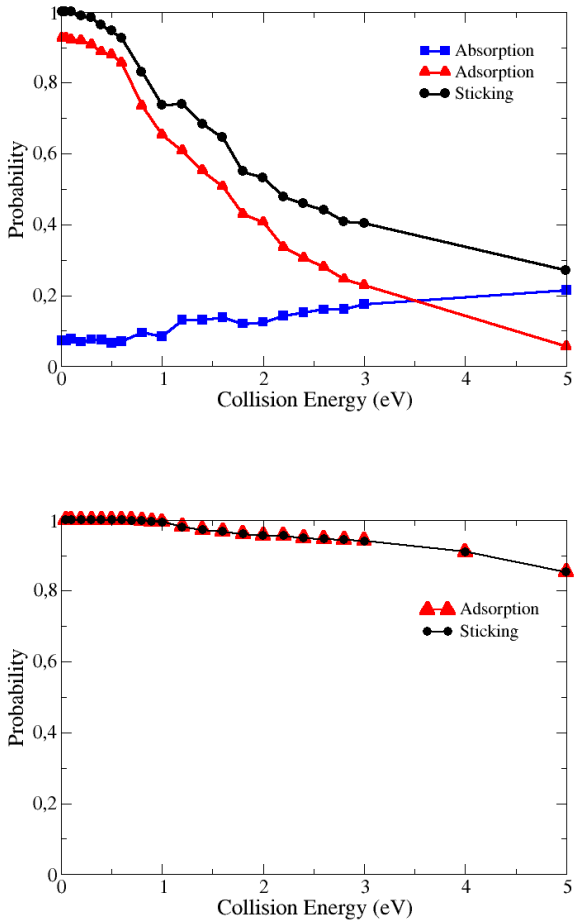

FIG. 4. Decomposition of the sticking probabilities in adsorption and absorption probabilities for H/W(100) (upper panel) and N/W(100) (lower panel) within the GLO-LDFA model at 300K.

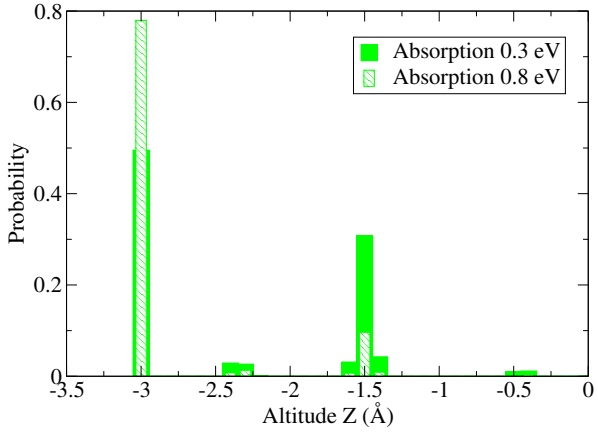

FIG. 5. Distribution of final altitudes for H-atoms absorbed into the bulk at 0.3 and 0.8 eV of collision energy. Simulations are done within the GLO-LDFA model with a surface temperature of 300K. The histogram at Z=−3.0 Å is not reflecting trajectories absorbed on a localized absorption site but rather hot atoms moving towards lower values of Z and penetrating into the bulk

Insights into the Adsorption and Absorption Processes

Within the low energy regime, an analysis of the final Z distribution of the absorbed H atoms reveals three sites of absorption below the top layer (see Fig. 5 where Z-distributions are plotted for 0.3 eV and 0.8 eV of initial collision energies). A detailed analysis allow us to locate those absorption sites on bridge site for the $Z = -0.40$ and -2.37 Å distances, and on top-to-bridge (T2B) site for $Z = -1.55$ Å.

Those 3 sites of absorption are thus populated at both 0.3 and 0.8 eV, for trajectories initiated with normal incidence to the surface. The most populated site is the T2B, especially at 0.8 eV, even if it is not the site characterized by the highest binding energy (see Table 1 for a comparison of the binding energy over the 3 adsorption sites). A non negligible proportion of the adsorbed atoms scatters into the bulk, as revealed by the histograms at Z=−3.0 Å, which altitude corresponds to the lowest altitude trajectories can reach in the simulations. In Table 1, mean energy losses are compared for trajectories ending into absorption sites, with an initial total energy of 0.3 eV. The mean energy loss which corresponds to those trajectories still in scattering is rather small (0.73 eV) leading to "hot atoms" characterized by mean total energy of about -0.43 eV, that is enough to overcome all the barriers to travel through the three first layers of the slab as can be seen on Fig. 6, where the potential energy as a function of the scattering path is depicted. The high energy regime is characterized by absorbed species still scattering into the bulk and none of them remains trapped into one of the 3 absorption sites identified at lower energies.

The scattering pathway into the bulk observed in the simulations is the Bridge-T2B-Bridge, as depicted in the Fig. 6. In short, the atoms that are neither reflected nor adsorbed penetrate the surface through the Bridge site and find the absorption site 1 (Bridge-1) and then migrate to site 2 (T2B) overcoming a barrier of 0.73 eV. The site 2 is the most populated for absorption, as mentioned above. Then, the H-atoms undergoes a migration to the site 3 (Bridge-3), with an activation barrier of 0.28 eV. Sites 1, 2, 3 shown in Fig. 7 correspond to tetrahedral interstitial sites (TIS), so we have found that motion of H-atoms into the bulk occurs along a TIS−TIS−TIS path as exhibited in Fig. 8 where (X, Y)-positions of the atoms scattering into the bulk are plotted for different Z altitudes. As can be seen in the figure, trajectories first concentrate around the TIS-bridge site when reaching the altitude corresponding to the site 1, then atomic positions spread out from bridge to TIS-T2B at altitude belonging to site 2. Finally, atoms end on TIS-bridge po-

sitions at the altitude of the site 3. Similar results have been reported by Liu *et al*[81]. In the present work, it was also found that atoms absorbed in any of the three sites can remain trapped. The lack of kinetic energy does not allow them to move out of their absorption site.

Interestingly, absorbed atoms are weakly bounded when compared to species adsorbed on the surface (E_{bind}= 3.08 eV), which makes this system a promising candidate for sub-surface recombination reactions with atoms coming from the gas phase. Results reported by Markejl *et al*[82] suggests there must be another recombination mechanism apart from Eley-Rideal surface recombination. Such a mechanism is characterized by a large exothermicity (of about 4 eV), producing vibrationally hot molecules. Exothermicity of Eley-Rideal path can not explain the highly hot molecules they observe. In our work, if one consider sub-surface recombination, with most of the exothermicity transferred to vibration motion, one could expect producing molecules excited until $v = 7$ vibrational state. Further simulation work would be required to study in details such sub-surface reactions.

As expected, the adsorption mechanism leads to H-atoms adsorbed on bridge site, whereas hollow site characterizes the adsorption of N-atoms. Reflection is a fast process decided rather quickly in less than two rebounds (a rebound is defined here as a sign change in the Z linear momentum), whereas adsorption mechanism (with 60 rebounds in average) and absorption (90 rebounds) mechanisms are characterized by a large number of rebounds. The "hot" absorbed atoms still scattering into the bulk follow a rather direct mechanism with a relatively small number of rebounds (around 10 rebounds) explaining the weak loss of energy experienced by the atoms in the latter case. Same kind of conclusions has been drawn for the N/W(100) with a fast direct reflection mechanism and an indirect mechanism of adsorption mediated through trapping and energy dissipation (around 30 rebounds).

The distribution of minimum distance reached by the atoms being either reflected, or adsorbed are represented on Fig. 9. As previously identified for H scattering on Au[37,38], the atomic adsorption follows a penetration/resurfacing mechanism for both H/W(100) and N/W(100). If we consider penetration to happen when the atom goes below $Z = 0$, roughly 60% of the H atoms adsorbed on W(100) has followed a penetration/resurfacing mechanism, against 15% for the N atoms case. In comparison, for H on Au(111) Janke *et al.*[38] found a penetration-resurfacing contribution of about 80% at 2.7 eV of incidence energy. At 0.8 eV, H-atoms can penetrate as deep as Z=−2 Å before resurfacing and being adsorbed on a bridge site of the surface. The loss of energy by electronic friction is enhanced by this penetration effect. For N-atoms, the penetration is somehow weaker since Z=−0.5 Å is only rarely reached at low collision energies. N/W(100) PES does not allow penetration of the atoms as easily as in the H-atoms case, and loss of

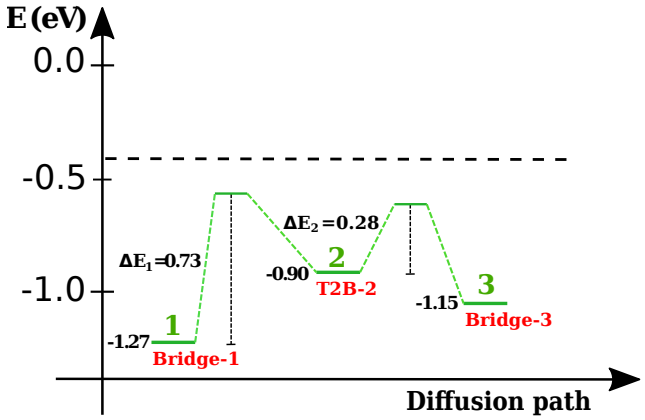

FIG. 6. Energetic scheme of the H-atoms in motion throughout the W(100) slab following the TIS-TIS-TIS pathway. Dashed line corresponds to the mean total energy of atoms reaching the -3.0 Å limit with a 0.3 eV of initial collision energy.

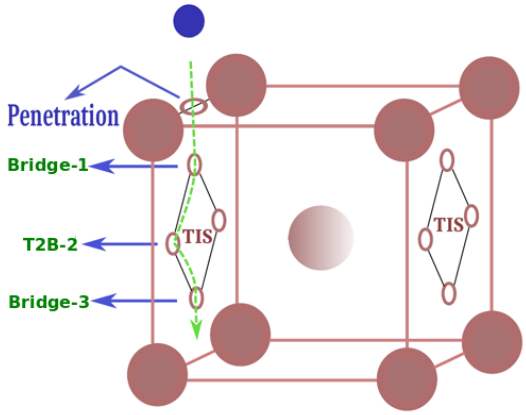

FIG. 7. Representation of the TIS-TIS-TIS pathway along sites 1, 2, and 3 within the W bcc unit cell. Projected onto (100) plane, site 1 corresponds to a bridge site, site 2 to a T2B site, and site 3 to a bridge.

Energy (eV)	Absorption sites, Z(Å)		
	−0.40	−1.55	−2.33
$\langle E_{loss} \rangle$	1.56	1.19	1.40
E_{bind}	1.27	0.90	1.15

TABLE I. Analysis of energy for absorption sites. The initial collision energy is 0.3 eV.

energy through coupling with the surface atoms motion is preventing any absorption even at energies higher than 2 eV (lowest energy barrier for absorption through the bridge site). In order to check this point, BOSS trajectories calculations have been performed for the N/W system. Within the BOSS approximation, where no energy exchange is allowed, all atoms approaching the surface at the vicinity of the bridge site with energies higher than 2 eV penetrate into the bulk reaching the Z=−3.0 Å limit.

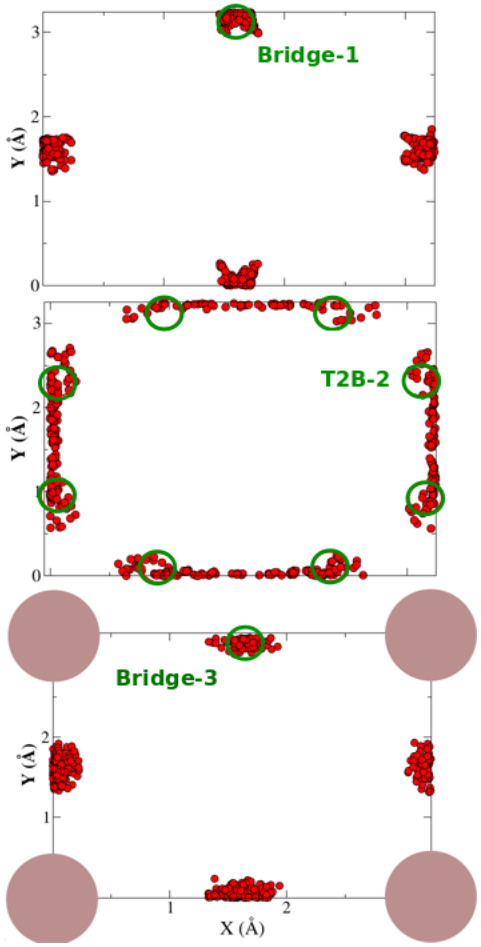

FIG. 8. X and Y distributions of atoms scattering into the bulk displayed for different values of Z that correspond to altitudes of site 1 (Z=-0.4 Å, upper panel), site 2 (Z=-1.55 Å, center panel), and site 3 (Z=-2.33 Å, lower panel).

As soon as GLO model is used in the simulations no more absorption is observed for the same conditions, exhibiting the strong influence of this energy loss channel. We have checked that the Z-limit used in the dynamics (Z=−3.0 Å) is low enough not to have any influence on the adsorption probability and the resurfacing mechanism.

Energy loss upon H reflection on W(100)

For several (111) *fcc* metal surfaces (i.e. Au, Pt, Ag, Pd, Cu, and Ni), comparison between theoretical simulations and atomic beam experiments has been performed[41] by considering energy loss spectra for H-atoms scattering back to the vacuum. In this work, H-atoms inelastic scattering has been analyzed for a high collision energy of 1.92 eV and off-normal incidence (initial angle of the beam with respect to the surface normal vector equal to 45°). It was found that the average energy loss is about 0.75 eV and very similar for all metals ranging from the lightest (Ni) to the heaviest surface

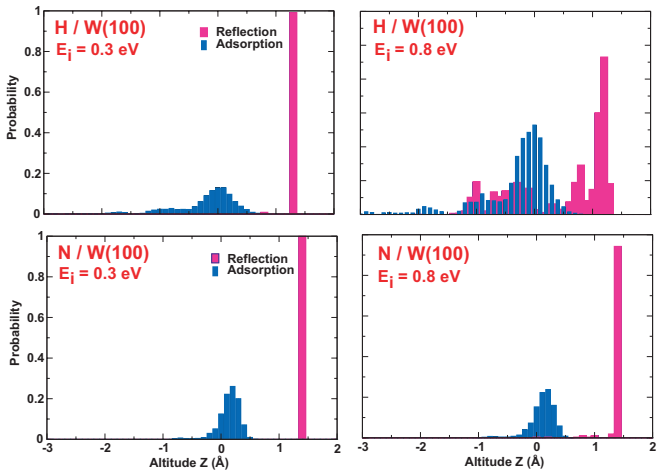

FIG. 9. Distributions of minimum altitudes reached by H-atoms (upper panel) and N-atoms (lower panel) either reflected, or adsorbed on the surface for two different initial collision energies (E_i): 0.3 and 0.8 eV within the GLO-LDFA model at 300K.

atoms (Au). Because the loss of energy is mainly due to electronic effects (that depend only weakly on the metal under study when compared to surface motion dissipation channel, where the mass is playing a key role), there is no significant change with the nature of the metal.

For comparison, the energy loss spectra of H scattering off the W(100) surface has been displayed in Fig. 10, for an initial energy of 1.92 eV and two incidence angles (normal incidence and off normal incidence with a polar angle of 45° taking an average over all azimuthal angles). In the off-normal case the mean energy loss is 0.8 eV in close agreement with previous work[41] on other metals. The shape of the energy loss spectrum exhibits three peaks, that can be attributed to reflections at different values of Z, roughly 1.2, -0.5, and -2 Å. As expected, the highest is the penetration of the atoms (i.e. the lowest altitude), the highest is the energy loss by electronic friction since atoms then travel in regions where electronic density is high. As a consequence, the third peak between 1.0 and 1.5 eV of energy loss is attributed to the reflection at lowest altitude i.e. $Z = -2$ Å. A comparison between normal and off-normal curves tends to show that incidence barely affect the energy loss. We also checked that sticking probability is weakly influenced by the incidence angle (calculations were made from normal incidence to 75° off-normal incidence). As a matter of fact the penetration to subsurface area is not influenced so much by the incidence angle since it often happens after long residence time at the vicinity of the surface where trapping mechanism dominates involving a significant loss of memory. The energy dissipation to the electrons of the surface follows total energy scaling (TES) process whatever if considering reflection, or sticking.

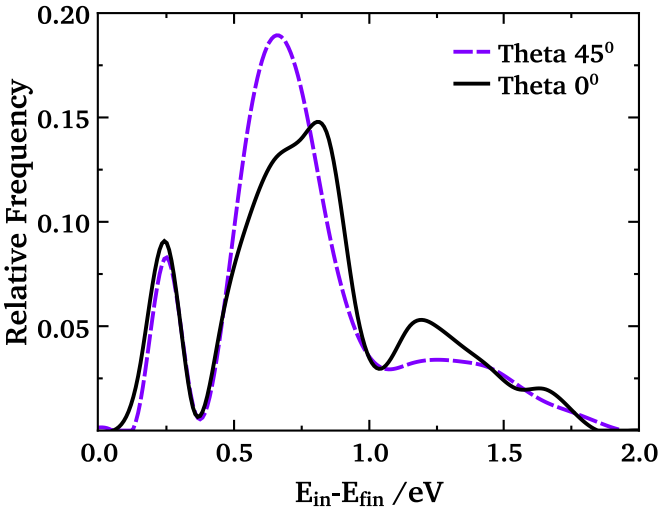

FIG. 10. Total energy loss spectra (in eV) of reflected atoms for an initial collision energy of 1.92 eV. Two values of incidence angles are reported (normal incidence and off normal incidence with a polar angle of 45 degrees averaged over all azimuthal angles). The distributions are normalized to the area. GLO-LDFA model.

IV. SUMMARY AND REMARKS

Scattering dynamics of H and N atoms on W(100) has been investigated by means of theoretical simulations. A special focus has been made on sticking mechanism discriminated into adsorption and absorption processes. As also demonstrated elsewhere[33,36–42], the H-atoms sticking is mediated through energy dissipation to electrons whereas coupling to lattice vibrations plays the major role for the case of N-atoms. H-atoms can penetrate the W slab through the bridge sites and either end absorbed on various sub-surface sites (bridge and T2B) between topmost and third layer, or scatter as hot atoms deeper into the bulk. The H-atoms motion between the top layer and the third layer of the slab occurs following a TIS−TIS−TIS path way. Part of the H-atoms adsorption mechanism follows the so-called penetration/resurfacing scheme already proposed in early works.[37] Sub-surface adsorbed H-atoms have been characterized and could potentially lead to recombination events with atoms coming from the gas phase, producing highly vibrationally excited molecules. Further theoretical works would be required to confirm this possible scenario.

Within the energy range considered in the simulations, the sticking of N-atoms is only described through the adsorption. No absorption is observed as the N/W(100) dynamics, strongly influenced by the loss of energy through lattice motion, prevents any penetration below -1.5 Å. For both H and N atoms the reflection is a direct process whereas sticking is characterized by indirect mechanisms involving many rebounds before the atoms remain thermalized on the surface. The energy loss spectra of the reflected back H-atoms has been studied, exhibiting total energy scaling behavior. The mean energy loss determined in our simulations is in close agreement with previous experimental and theoretical works on H scattering on several *fcc* metal (111) surfaces (Ni, Cu, Pd, Ag, Au, Pt). Therefore, our theoretical predictions for a (100) surface of a *bcc* metal reinforce this general feature of the electronically nonadiabatic adsorption process of atomic H on metals[37]. Further studies would be required to fully understand the features of the energy loss spectra in relation with surface structure and symmetry.

Acknowledgments

This work was conducted in the scope of the transborder joint Laboratory QuantumChemPhys: Theoreti- cal Chemistry and Physics at the Quantum Scale (ANR-10- IDEX-03-02).Computer time was provided by the Pole Modelisation computing facilities of the Institut des Sciences Moleculaires (UMR5255, CNRS/U. Bordeaux), partly funded by the Nouvelle Aquitaine Region

[1] I. Langmuir, *J. Am. Chem. Soc.*, 1912, **34**(10), 1310–1325.
[2] M. Andersson, F. Abild-Pedersen, I. Remediakis, T. Bligaard, G. Jones, J. Engbæk, O. Lytken, S. Horch, J. Nielsen, J. Sehested, J. Rostrup-Nielsen, J. Nørskov, and I. Chorkendorff, *J. Catal.*, 2008, **255**(1), 6 – 19.
[3] A. Nilsson, L. G. M. Petersson, , and J. K. Nørskov, *Chemical Bonding at Surface and Interfaces*, Elsevier, Amsterdam, 2008.
[4] G. A. Somorjai, *Introduction to Surface Chemistry and Catalysis*, Wiley, New York, 1994.
[5] I. Chorkendorff and J. W. Niemantsverdriet, *Concepts of Modern Catalysis and Kinetics*, Wiley-VCH, Weinheim, 2003.
[6] G. Ertl, *J. Vac. Sci. Technol. A*, 1983, **1**, 1247.
[7] K. Honkala, A. Hellman, I. N. Remediakis, A. Logadottir, A. Carlsson, S. Dahl, C. H. Cristensen, and J. K. Nørskov, *Science*, 2005, **307**, 55.
[8] I. Takagi, S. Nomura, T. Minamimoto, M. Akiyoshi, T. Kobayashi, and T. Sasaki, *J. Nucl. Mat.*, 2015, **463**, 1125 – 1128.
[9] K. Heinola, T. Ahlgren, K. Nordlund, and J. Keinonen, *Phys. Rev. B.*, 2010, **82**, 094102.
[10] D. Terentyev, V. Dubinko, A. Bakaev, Y. Zayachuk, W. V. Renterghem, and P. Grigorev, *Nucl. Fusion*, 2014, **54**(4), 042004.
[11] H.-B. Zhou, Y.-L. Liu, S. Jin, Y. Zhang, G. Luo, and G.-H. Lu, *Nucl. Fussion*, 2010, **50**(2), 025016.
[12] M. Capitteli, *NATO ASI Ser., C, Kluwer Academic Publishers Dordrecht*, 1989, **482**.
[13] M. Cacciatore, M. Rutigliano, and G. D. Billing, *J. Thermophys Heat Transfer*, 1999, **13**, 195.
[14] D. Bruno, M. Cacciatore, S. Longo, and M. Rutgliano, *Chem. Phys. Lett.*, 2000, **320**, 245.
[15] L. Bedra, M. Rutigliano, M. Balat-Pichelin, and M. Cacciatore, *Langmuir*, 2006, **22**, 7208.
[16] M. Rutigliano, A. Pieretti, M. Cacciatore, N. Sanna, and V. Barone, *Surf. Sci.*, 2006, **600**, 4239.
[17] N. Perron, N. Pineau, E. Arquis, J. C. Rayez, and A. Salin, *Surf. Sci.*, 2005, **599**, 160.
[18] C. Arasa, P. Gamallo, and R. Sayos, *J. Phys. Chem. B.*, 2005, **109**, 14954.
[19] L. Bedra, M. J. H. Balat-Pichelin, M. Rutigliano, and M. Cacciatore, *AIP Conf. Proc.*, 2005, **762**, 1037.
[20] E. J. Jumper and W. A. Seward, *J. Thermophys. Heat Transfer*, 1991, **5**, 284.
[21] R. J. Willey, *J. Thermophys. Heat Transfer*, 1993, **7**, 55.
[22] O. Deutschmann, U. Riedel, and J. Warnatz, *J. Heat Transfer*, 1995, **117**, 495.

[23]S. Reggiani, M. Barbato, C. Bruno, and J. Muylaert, *J. Thermophys. Heat Transfer*, 2000, **14**, 412.
[24]T. Kurotaki, *AIAA paper*, 2000, p. 2366.
[25]B. Halpern and D. E. Rosner, *J. Chem. Soc., Faraday Trans.*, 1978, **74**, 1883.
[26]B. van Ootegem, D. Conte, N. Sauvage, P. Tran, P. Vervisch, A. Desportes, P. Regnier, C. Crespos, P. Larregaray, J. C. Rayez, E. Arquis, and N. Perron, *4th International Symposium on Atmospheric Vehicles and Systems*.
[27]M. Balat-Pichelin, M. Czerniak, and J. M. Badie, *J. Spacecr. Rockets*, 1999, **36**, 273.
[28]M. Balat-Pichelin, M. Czerniak, and J. M. Badie, *Appl. Surf. Sci.*, 1997, **120**, 225.
[29]V. Moron, P. Gamallo, L. Martin-Gondre, C. Crespos, P. Larregaray, and R. Sayos, *Phys. Chem. Chem. Phys.*, 2011, **13**, 17494.
[30]V. Moron, L. Martin-Gondre, C. Crespos, P. Larregaray, P. Gamallo, and R. Sayos, *Comp. Theo. Chem.*, 2012, **990**, 132.
[31]L. Martin-Gondre, M. Alducin, G. A. Bocan, R. Díez-Muiño, and J. I. Juaristi, *Phys. Rev. Lett.*, 2012, **108**(9), 096101.
[32]L. Martin-Gondre, G. A. Bocan, M. Alducin, J. I. Juaristi, and R. Díez-Muiño, *Comp. Theo. Chem.*, 2012, **990**, 126–131.
[33]M. Blanco-Rey, J. I. Juaristi, R. Díez Muiño, H. F. Busnengo, G. J. Kroes, and M. Alducin, *Phys. Rev. Lett.*, 2014, **112**, 103203.
[34]H. F. Busnengo, M. A. Di Césare, W. Dong, and A. Salin, *Phys. Rev. B*, 2005, **72**(12), 125411.
[35]J. I. Juaristi, M. Alducin, R. D. Muino, H. F. Busnengo, and A. Salin, *Phys. Rev. Lett.*, 2008, **100**, 116102.
[36]J. Nørskov and B. Lundqvist, *Surf. Sci.*, 1979, **89**(1), 251 – 261.
[37]O. Bünermann, H. Jiang, Y. Dorenkamp, A. Kandratsenka, S. M. Janke, D. J. Auerbach, and A. M. Wodtke, *Science*, 2015, **350**(6266), 1346–1349.
[38]S. M. Janke, D. J. Auerbach, A. M. Wodtke, and A. Kandratsenka, *J. Chem. Phys.*, 2015, **143**(12), 124708.
[39]M. Pavanello, D. J. Auerbach, A. M. Wodtke, M. Blanco-Rey, M. Alducin, and G.-J. Kroes, *J. Phys. Chem. Let*, 2013, **4**(21), 3735–3740.
[40]G.-J. Kroes, M. Pavanello, M. Blanco-Rey, M. Alducin, and D. J. Auerbach, *J. Chem. Phys.*, 2014, **141**(5), 054705.
[41]Y. Dorenkamp, H. Jiang, H. Köckert, N. Hertl, M. Kammler, S. M. Janke, A. Kandratsenka, A. M. Wodtke, and O. Bünermann, *J. Chem. Phys.*, 2018, **148**(3), 034706.
[42]M. A. Zeb, J. Kohanoff, D. Sánchez-Portal, A. Arnau, J. I. Juaristi, and E. Artacho, *Phys. Rev. Lett.*, 2012, **108**, 225504.
[43]R. Pitts, A. Kukushkin, A. Loarte, A. Martin, M. Merola, C. Kessel, V. Komarov, and M. Shimada, *Phys. Scr.*, 2009, **138**, 014001.
[44]N. Fernandez, Y. Ferro, and D. Kato, *Acta Mater.*, 2015, **94**, 307 – 318.
[45]Y. Liu, H. Z. Y. Zhang, F. L. G.H. Lu, and G. Luo, *Phys. Rev. B.*, 2009, **79**, 172103.
[46]K. Heinola and T. Ahlgren, *J. Appl. Phys.*, 2010, **107**, 113531.
[47]D. Johnson and E. Carter, *J. Mater. Res.*, 2010, **25**, 315.
[48]W. Shu, E. Wakai, and T. Yamanishi, *Nucl. Fusion*, 2007, **47**(3), 201.
[49]O. Galparsoro, R. Pétuya, H. Busnengo, J. Juaristi, C. Crespos, M. Alducin, and P. Larregaray, *Phys. Chem. Chem. Phys.*, 2016, **18**, 31378–31383.
[50]O. Galparsoro, H. F. Busnengo, A. E. Martinez, J. I. Juaristi, M. Alducin, and P. Larregaray, *Phys. Chem. Chem. Phys.*, 2018, **20**, 21334–21344.
[51]O. Galparsoro, R. Pétuya, J. Juaristi, C. Crespos, M. Alducin, and P. Larregaray, *J. Phys. Chem. C.*, 2015, **119**(27), 15434–15442.
[52]G. Volpilhac, H. F. Busnengo, W. Dong, and A. Salin, *Surf. Sci.*, 2003, **544**, 329–338.
[53]J. Strömquist, L. Bengtsson, M. Persson, and B. Hammer, *Surf. Sci.*, 1998, **397**(1), 382 – 394.
[54]W. Kohn and L. J. Sham, *Phys. Rev.*, 1965, **140**, A1133.
[55]P. Hohenberg and W. Kohn, *Phys. Rev.*, 1964, **136**, 864.
[56]K. Lee, E. D. Murray, L. Kong, B. I. Lundqvist, and D. C. Langreth, *Phys. Rev. B.*, 2010, **82**, 081101.
[57]A. Peña-Torres, H. F. Busnengo, J. I. Juaristi, P. Larregaray, and C. Crespos, *Phys. Chem. Chem. Phys.*, 2018, **20**(29), 19326–19331.
[58]A. Pena-Torres, H. F. Busnengo, J. I. Juaristi, P. Larregaray, and C. Crespos, *J. Phys. Chem. C.*, 2019, **123**(5), 2900–2910.
[59]D. Migliorini, F. Nattino, and G.-J. Kroes, *J. Chem. Phys.*, 2016, **144**(8), 084702.
[60]L. Martin-Gondre, J. I. Juaristi, M. Blanco-Rey, R. D. Muiño, and M. Alducin, *J. Chem. Phys.*, 2015, **142**(7), 074704.
[61]H. F. Busnengo, A. Salin, and W. Dong, *J. Chem. Phys.*, 2000, **112**(17), 7641–7651.
[62]R. A. Olsen, H. F. Busnengo, A. Salin, M. F. Somers, G. J. Kroes, and E. J. Baerends, *J. Chem. Phys.*, 2002, **116**, 3841.
[63]G. Kresse, *Phys. Rev. B.*, 2000, **62**, 8295.
[64]A. D. Becke, *Phys. Rev. A*, 1988, **38**, 3098.
[65]J. P. Perdew, *Phys. Rev. B*, 1986, **33**, 8822.
[66]D. Vanderbilt, *Phys. Rev. B (Rapid Communication)*, 1990, **41**, 7892.
[67]K. Laasonen, R. Car, C. Lee, and D. Vanderbilt, *Phys. Rev. B (Rapid Communication)*, 1991, **43**, 6796.
[68]K. Laasonen, A. Pasquarello, C. Lee, R. Car, and D. Vanderbilt, *Phys. Rev. B*, 1993, **47**, 10142.
[69]J. Hafner and G. Kresse, in *Properties of Complex Inorganic Solids*, ed. A. Gonis, A. Meike, and P. E. A. Turchi, Springer US, Boston, MA, 1997; pp. 69–82.
[70]G. Kresse and J. Hafner, *Phys. Rev. B.*, 1993, **47**, 558.
[71]G. Kresse and J. Hafner, *Phys. Rev. B.*, 1993, **48**, 13115.
[72]G. Kresse and J. Furthmuller, *Comput. Mater. Sci.*, 1996, **6**, 15.
[73]G. Kresse and J. Furthmuller, *Phys. Rev. B.*, 1996, **54**, 11169.
[74]F. Nattino, O. Galparsoro, F. Costanzo, R. Diez Muino, M. Alducin, and G. Kroes, *J. Chem. Phys.*, 2016, **144**, 244708.
[75]H. F. Busnengo and A. E. Martinez, *J. Phys. Chem. C*, 2008, **112**, 5579–5588.
[76]M. R. Barnes and R. F. Willis, *Phys. Rev. Lett.*, 1978, **41**(25), 1729–1733.
[77]P. Alnot, A. Cassuto, and D. A. King, *Surf. Sci.*, 1989, **215**, 29–46.
[78]C. Ibarguen, P. Larregaray, A. Peña-Torres, and C. Crespos, *J. Phys. Chem. C*, 2018, **122**(50), 28856–28861.
[79]D. Novko, M. Blanco-Rey, J. I. Juaristi, and M. Alducin, *Phys. Rev. B*, 2015, **92**, 201411.
[80]D. Novko, M. Blanco-Rey, J. I. Juaristi, , and M. Alducin, *Phys. Rev. B*, 2016, **93**, 245435.
[81]Y.-N. Liu, T. Wu, Y. Yu, X.-C. Li, X. Shu, and G.-H. Lu, *J. Nucl. Mater.*, 2014, **455**(1-3), 676–680.
[82]S. Markelj and I. Cadez, *J. Chem. Phys.*, 2011, **134**, 124707.